TIRE-PAVEMENT INTERACTION NOISE OF CONCRETE PAVEMENTS

A DISSERTATION
SUBMITTED TO THE FACULTY OF THE GRADUATE SCHOOL
OF THE UNIVERSITY OF MINNESOTA
BY

Bernard Igbafen Izevbekhai

IN PARTIAL FULFILLMENT OF THE REQUIREMENTS
FOR THE DEGREE OF
DOCTOR OF PHILOSOPHY

PROFESSOR LEV KHAZANOVICH (Advisor)
PROFESSOR VAUGHAN R. VOLLER (Advisor)

UNIVERSITY OF MINNESOTA

JULY 2012

ACKNOWLEDGEMENTS

I am grateful to Dr. Paul Donavan (Illingworth & Rodkin), Dr. Rob Rasmussen (Transtec), Professor Ulf Sandberg (VTI, Sweden), Professor Andy Seybert (University of Kentucky) and Professor W. James Wilde (Minnesota State University) for their invaluable intellectual resources. I acknowledge Minnesota Department of Transportation for encouraging my intellectual development and for providing the MnROAD research facility for this research work. In that regard, appreciation is especially due to Doug Schwartz (Retired) Maureen Jensen and Keith Shannon of the MnDOT Office of Materials and Roads Research for their support, mentoring and provision of some tuition reimbursement for the program. Alexandra Akkari, Tim Nelson and Dan Franta are specially acknowledged. I am indebted to my instructors at the Infrastructure Systems Engineering program / Transportation Leadership Institute, particularly Professor Vaughan Voller, Professor Eugene Skok and Professor Tom Maze (now deceased) and Professor Karl Smith whose teaching method was very inspiring. I am grateful to my instructors/ examiners in the doctorate degree program particularly Professor Rajesh Rajamani, Professor Mihai Marasteanu and Professor Randal Barnes. I acknowledge my advisors Professor Lev Khazanovich and Professor Vaughan Voller for the tireless reviews as well as generous provision of poignant, enriching and edifying guidance.

I am indebted to my children: Jed, Kevin, Eliel and Elianna for all their encouragement and perseverance with me through the program. This program would not have been possible without the support of my loving wife, Dora who made remarkable sacrifices to accommodate incessant and prolonged burning of the midnight oil.
Most importantly, I am unequivocally grateful to the Almighty God whose grace and favor surmounted unusual and inexplicable challenges and facilitated successful completion of this endeavor.

DEDICATION

The quintessence of de-facto human innovation, invention or intervention accentuates only a microcosm, nay a mere infinitesimal pittance of God's creative ingenuity. This doctoral thesis is dedicated to the Almighty God who is the embodiment of absolute knowledge.

Unequivocal obeisance is hereby paid to His infinite majesty.

ABSTRACT

Vehicles generate noise through their power-train, aerodynamics, exhausts systems and tire pavement interaction. Of these sources, tire pavement interaction is by far the most dominant source at regular cruising highway speeds. A standard means of mitigating the environmental hazards of freeway traffic noise is through the use of noise abatement walls. Such infrastructure, however, can be very expensive and difficult to maintain. Hence the objective of this thesis is to investigate the possibility of reducing traffic noise associated with tire pavement interactions through pavement surface modification.

This work was focused on an investigation of pavement surfaces to determine what texture variables affect pavement noise and examine ways of modifying these to improve pavement quietness. The first step was the identification and physical conceptualization of possibly significant noise inducing variables with an emphasis on pavement surface texture. This resulted in a hypothesized model-form for predicting of noise related to tire pavement interactions. It was followed by a large scale field campaign that performed numerous on-board sound intensity (OBSI) measurements on various texture types under various atmospheric conditions. These measurements along with the proposed model-form were then used in an unforced stepwise regression process. It was ascertained that asperity interval (a measure of texture wavelength), texture direction relative to the traffic direction, and texture spikiness (a measure of the probability density function of the texture amplitude) were the major surface finish contributors to tire pavement noise. Contrary to previously held belief, however, the profile depth was not identified as a significant surface finish texture variable. This analysis also identified air temperature and pavement ride quality (measured through the international roughness index IRI) as the significant non-textured contributors to tire pavement interaction noise.

The complete regression analysis resulted in a model for predicting OBSI from measurable pavement surface variables, air temperature and ride quality. This model was able to reproduce over 90% of the field measurements to within 1.5 dBA which is the band of the typical human noise detection. It was consequently used to determine the optimum surface texture for a quiet pavement. In addition, the model was used to predict the OBSI for the design of two large scale pavement rehabilitation projects. Moreover, the design pavement texture resulted in a post-construction noise level drop of approximately 5 dBA. The predicted OBSI pre-construction and post-construction were within 1 dBA of the field measurements.

TABLE OF CONTENTS

ACKNOWLEDGEMENTS i

DEDICATION ii

ABSTRACT iii

TABLE OF CONTENTS v

LIST OF TABLES ix

LIST OF FIGURES x

NOTATION & ACRONYMS xii

CHAPTER 1: INTRODUCTION 1

1.1: MOTIVATION 1

1.2: OBJECTIVE AND APPROACH 2

CHAPTER 2: CHARACTERISTICS OF PAVEMENT SURFACES 4

2.1: CHAPTER INTRODUCTION 4

2.2: SURFACE TEXTURE TYPES 4

2.2.1: Texturing at Various Stages of Concrete Maturity…….. 4

2.2.2: Textures Established in Freshly Placed Concrete …… 5

2.2.3: Textureing Semi Hardened Concrete: Exposed Aggregate…... 6

2.2.4: Textures Established in Hardened concrete …..……. 8

2.3: FEATURES OF PAVEMENT SURFACES 9

2.3.1: Microtexture and Megatexture 9

2.3.2: Characterizing Smaller Scale Pavement Surface Features……. 10

2.3.3: Characterizing Larger Scale Pavement Surface Features…….. 15

2.4: MEASUREMENT OF TEXTURE PARAMETERS 16

2.4.1 Measurement of Small Scale Features……. 16

2.4.2: Measurement of Large Scale Texture Properties…… 18

2.5: STANDARD REFERENCE TEST TIRE 19

2.6: CHAPTER SUMMARY..... 21

CHAPTER 3: THE TIRE PAVEMENT NOISE MODEL..... 23

3.1 CHAPTER INTRODUCTION..... 23

3.2: WHAT IS NOISE? 23

3.3: THE PROPOSED MODEL FORM..... 25

3.4: INTRINSIC TIRE NOISE..... 26

3.5: TIRE PAVEMENT NOISE..... 27

3.5.1: Scales of Texture……... 27

3.5.2: Larger Scale Texture Effects: ……. 28

3.5.3: Smaller Scale Texture……. ….. 29

3.6: THE FINAL MODEL FORM 34

CHAPTER 4: MEASUREMENT OF OBSI 37

4.1: CHAPTER INTRODUCTION..... 37

4.2: THE OBSI SET-UP AND USE IN THE TIRE PAVEMENT NOISE EXPERIMENT 38

4.3: OBSI DATA 43

CHAPTER 5: FITTING THE MODEL 54

5.1 CHAPTER INTRODUCTION 54

5.2: OVERVIEW OF STEPWISE REGRESSION METHOD 55

5.3: RESULTS 56

5.4: COMPARISON OF PREDICTED OBSI RANGE OF MODEL COMPONENTS. 61

5.5: VALIDATION OF NORMALITY & HOMOSCEDASTICITY 63

5.6: POWER OF MODEL 64

5.7: CHAPTER SUMMARY 66

CHAPTER 6: IMPACT OF SURFACE TEXTURE ON NOISE 68

6.1: STRATEGY 68

6.2: CHAPTER SUMMARY 71

CHAPTER 7: APPLICATION OF THE MODEL IN REHABILITATING A SURFACE TO REDUCE NOISE 72

7.1: BRIEF BACKGROUND 72

7.2: VALIDATION PROCESS 72

7.3 CHAPTER SUMMARY 76

CHAPTER 8: CONCLUSION & RECOMMENDATIONS 78

8.1 SUMMARY OF RESEARCH EFFORTS 78

8.2: SPECIFIC CONTRIBUTIONS OF THIS RESEARCH 78

8.3: CONCLUSIONS 79

8.4: RECOMMENDATIONS 81

8.5: LIMITATIONS OF THE STUDY 81

REFERENCES 83

APPENDIX 89

SOUND SOURCE AND ACOUSTIC MEDIA 89

APPENDIX 1A: ENVIRONMENTAL EFFECTS ON ON-BOARD-SOUND-INTENSITY LEVELS DERIVED FROM THE RESPONSE OF AN ACOUSTIC MEDIUM TO A PULSATING SOURCE IN CONTACT 89

APPENDIX 1B: PRINCIPLES OF NEAR FIELD MICROPHONES (ACTIVE VS REACTIVE NOISE) 95

LIST OF TABLES

TABLE 2.1: Starting Variables..... 13

TABLE 2.2: Different Texture Configurations 17

TABLE 2.3: Example. IRI Summary for a Section Measured 8/9/07 19

TABLE 4.1: Typical OBSI Output from One Run. 43

TABLE 4.2: Distinct Texture Configurations 45

TABLE 4.3: Descriptive Statistics of the 433 Sample Space OBSI Data 47

TABLE 4.4a: Configuration 1a Transverse Tine..... 48

TABLE 4.4b: Configuration 1b Transverse Tine 49

TABLE 4.4c: Configuration 2 Conventional Grind 50

TABLE 4.4d: Configuration 3 Innovative Grind..... 51

TABLE 4.4e: Configuration 3*: Ultimate Innovative Grind..... 51

TABLE 4.4f: Configuration 4: Exposed Aggregate Texture..... 52

TABLE 4.4g: Configuration 5a. Longitudinal Drag Texture 52

TABLE 4.3h: Configuration 5b: Transverse Drag Texture 53

TABLE 5.2: Coefficients, P-Values and Adjusted R^2 of Final Model 57

TABLE 5.3: Effect of Component Variable on the Model..... 62

TABLE 6.1: The Dominant Configuration Dimensions in the Model 69

TABLE 7.1: Pre-Grind Measurements. 73

TABLE 7.2: Model Prediction versus Measured OBSI Pre-Grind..... 74

TABLE 7.3: Texture Design For Grinding..... 75

LIST OF FIGURES

FIGURE 2.1: Fresh Concrete Texturing 6

FIGURE 2.2: Method of Creating Textures in Semi Hardened State: Exposed Aggregate Finish 7

FIGURE 2.3: Method of Creating Textures in Hardened State: Diamond Grind 9

FIGURE 2.4: Magnified (X100) Cross Section Through a Drag Texture Indicating Definite Configuration Patterns. 11

FIGURE 2.5: Layout and Probability Density Function of Spiky and Non-Spiky Textures 13

FIGURE 2.6: Circular Track Meter ASTM E-2157 (ASP and SP) 17

FIGURE 2.7: Lightweight Profiler 18

FIGURE 3.1: Major Tire Texture Noise Mechanisms: Tire Pavement Tread Block and Air-Compression Noise 30

FIGURE 4.1: Left Statistical Pass-By, Right: Close proximity (CPX) Method 38

FIGURE 4.2: Layout (Set up of Experiment OBSI Test Tire, Rig and Communication Assembly) 40

FIGURE 4.3: Layout of Microphones with Respect to Contact Patch 41

FIGURE 4.4: Schematics of OBSI Set-up (Analyzer and Computer in Vehicle) 42

FIGURE 4.5: Cumulative Percentile OBSI Data Measured (Data Currently Includes IRI and Temp Effects) 46

FIGURE 5.1: Fitted Model (1.5 dB Offset Enclosed 92% of the data) 59

FIGURE 5.2: Model Obtained by Using Asperity Groove width in Lieu of Asperity Interval 60

FIGURE 5.3: Homoscedasticity Validation in the Model 64

FIGURE 5.4: Homoscedasticity Validation in the Model 64

FIGURE 6.1: Predicted Vs. Measured OBSI at IRI of 1 m/km and Temperature of 293 degree K 70

FIGURE 7.1: The Quiet 2010 Ultimate Grind and the Pre-Grind Transverse Tine 76

FIGURE A1. 1: Normalized Sound Intensity Due to Atmospheric pressure at MnROAD for Temperature of 293 degrees K. 93

FIGURE A1.2: Relative Humidity Effects on Normalized SI 94

NOTATION & ACRONYMS

A	Amplitude of acoustic vibration or oscillation
A	Area particularly of a sphere around a sound source
A- Weighting	Weighted scale of human hearing (ref sound intensity: 10^{-12} watts/m^2)
ASP	Asperity interval
ASPGW	Asperity groove width
ATD	Astro turf drags texture
B	Bulk modulus of acoustic medium
CDG	Conventional diamond ground texture
CTM	Circular track meter ASTM E-2157 Standard laser equipped device for measurement of texture depth
dB	Decibel, a measure of sound intensity
dBA	Decibel A, a measure of sound intensity in the A- weighted scale referenced to human hearing threshold (10^{-12} Watts/m^2)
DG	Diamond ground texture
DIR	Texture direction. transverse =1, longitudinal =0
ESS	Estimated sum of squared errors.
ETD	Estimated texture depth. Mean texture depth from a high-speed or friction device (mm)
Ha	Alternate Hypothesis
Ho	Null Hypothesis
IDG	Innovative diamond ground texture
IRI	International roughness index: International measurement of pavement smoothness (inches/mile) (m/km)
K	Wave number
MTD	Mean texture depth: Mean texture depth determined from the sand volumetric technique (SVT) process.

MPD	Mean profile depth: Mean texture depth measured with ASTM E-2157
N, n	Population or number of terms
OBSI	On board sound intensity. Log sum of sound intensity recorded at 12 designated third-octave frequencies. AASHTO TP 76-08
SP	Texture spikiness variable positive =1 and negative =0
PSD	Power spectral density: An expression of the dominance of certain frequencies when measured values are raised to the second power and plotted against the frequency or wavelength.
P	Pressure/ atmospheric pressure
P-Value	Evidence against the null hypothesis (Ho). In regression where Ho means no effect, a small value of P: ($P<<\alpha$) characterizes a significant variable
R^2	Coefficient of determination: (goodness of fit) is the percentage or ratio of the data explained by a model.
R^2 (Adjusted)	Adjusted coefficient of determination: (goodness of fit). Measure of goodness of fit that is not biased by number of variables unless those variables are significant. Only addition of significant variables improve the model
SEE	Standard error of estimate
SR	Surface rating: A number from 0 to 4 that indicates the extent of visible surface distress. (Number 4 represents a pavement in good condition)
SRTT	Standard reference test tire ASTM F2493 - 08
SVT:	Sand volumetric technique (Sand patch test) ASTM E-965 Measurement technique for MTD using glass beads.
T	Air temperature (degree Kelvin)
TPIN	Tire Pavement Interaction noise
TSS	Total Sum of Square Errors
TT	Transverse tined texture

"Type I" Error:	The null hypothesis is right and the model does not say so (false alarm).
"Type II" Error:	The null hypothesis is wrong and the model says it is wrong (failed alarm)
V	Volume
w	Angular Speed
X	General direction of acoustic propagation
Y	Asperity height variability
α	Probability of a "Type I" error: Threshold for P-value
β	Probability of a "Type II" error, measure of power of a regression or model

CHAPTER 1: INTRODUCTION

1.1: MOTIVATION

Pavements are designed for structural capacity mainly to enable them carry traffic loads, withstand environmental factors, and provide safe and affordable transportation at reasonable cost. Very often pavements are rehabilitated, not for structural capacity needs, but because of functional performance issues. Functional performance variables include friction, ride quality and traffic noise. The focus of the research is the latter, i.e., traffic noise or more particularity, noise resulting from tire pavement interactions on concrete pavements.

Tire pavement interaction noise is the acoustic signal generated when the tire of a moving vehicle interacts with the pavement surface. At speeds of around 30 miles per hour the noise from tire pavement interactions account for half of the total traffic noise [1.1]. At freeway speeds, it is by far the dominant source accounting for 80% of the overall noise [1.2]. Additionally, health risks associated with traffic noise have been identified and documented [1.3]. In their publication Sorenson et al showed that the likelihood of stroke in the older population was tremendously increased by exposure of the older population to traffic noise.

Currently the most common method of abating traffic noise is through the use of noise walls. Noise walls, along with other noise barrier types such as sound berms, are exterior structures designed to protect sensitive land uses from noise pollution [1.4]. Unfortunately, noise abatement walls are fraught with the demerits of high cost, obliteration of scenic view and increased right-of-way requirements [1.4] [1.5]. The United States Department of Transportation [1.6] reported that the cost of walls ranged from $18 per square foot to $31 per square ft. This brings the average cost of a noise wall built to a standard 20-ft height to a range of $1.9 - 3.3 million per mile. This additional

road project cost is increased by right of way requirements and other intangibles such as access minimization and impediment to drainage. In addition to cost, such walls could also have undesirable consequences on sound levels. For example, through a shadow effect, some walls can cause a thermal inversion that will increase the intensity of the noise source at the pavement surface [1.5].

Another means of reducing the traffic noise is to directly develop quieter pavement designs [1.7]. Towards this end, the United States Department of Transportation [1.8] has initiated the quiet pavement pilot projects (QPPP) and the quiet pavement research (QPR) programs [1.8] where some concerted efforts have been made particularly in characterizing far-field measurements [1.9]. These earlier initiatives were challenged by the absence of a suitable body of knowledge of factors associated with tire pavement interaction noise.

Consequently, the central thesis in this work is that to be successful such initiatives need to be aimed at developing validated relationships between surface features in a pavement and the noise generated via its interactions with tires. Modifications of the surface finish of an existing pavement are typically in the price range of $0.1 million per lane-mile; a cost that is well below the cost of a sound wall. Hence, ability to quantitatively link surface texture to tire pavement noise may lead to successful and cost-effective noise abatement along with the additional benefit of improved pavement function.

1.2: OBJECTIVE AND APPROACH

The overall objective is to develop a model to predict tire-pavement noise and use this model to identify optimum surface finishes for concrete pavements. In arriving at this objective the key tasks are:

- A characterization of pavement surfaces, both small scale features related to texture and the larger scale features that influence ride quality.

- The identification of possible contributors to tire-pavement noise towards proposing a model form for prediction.

- The development and application of a robust protocol for collecting tire-pavement noise data in the field.

- The use of this data, with the proposed model-form to arrive at a model for predicting tire-pavement interaction noise from surface texture, ride quality and environmental (air temperature) inputs.

- An analysis of the components of the model along with an identification of the quietest pavement texture.

- The use and validation of the model in actual construction projects.

CHAPTER 2: CHARACTERISTICS OF PAVEMENT SURFACES

2.1: CHAPTER INTRODUCTION

In Chapter 1, reference was made to the importance of ascertaining the factors that influence tire pavement noise. Therefore, it is expedient in this chapter to examine typical surface texture types and more importantly, general properties of concrete pavement surface configurations that may affect tire pavement noise.

A freshly placed concrete pavement is usually frictionless and void of significant asperities until the surface is textured. This chapter discusses the methods used to create various textures, the typical geometric features that characterize them and the ways in which these features can be measured.

2.2: SURFACE TEXTURE TYPES

A discussion of texture types can be approached from the various categorizations of texture types, their configuration and their construction. Surface texture types are mainly named by the method in which they are produced or constructed. In this subsection therefore, the texture types will be categorized first by their method of construction and subsequently by their geometric dimensions.

2.2.1: Texturing at Various Stages of Concrete Maturity

Concrete pavements are textured either in their fresh/green, semi-hardened, or hardened condition. They are discussed below.

2.2.2: Textures Established in Freshly Placed Concrete

Fresh concrete texturing methods follow immediately after concrete placement and finishing when the concrete is still green/plastic. The texture types include turf/ broom/burlap drag and tining.

Drag textures are established by dragging a loaded, inverted turf broom or burlap across or along the finished concrete surface. The turf broom or burlap is transversely dragged when the direction of texturing is perpendicular to the driving direction and longitudinally when the inverted turf/ broom or burlap is dragged along the direction of travel. In all cases, to ensure uniformity of the pressure on the turf to produce uniform texture, a uniformly distributed load is placed on the turf / broom/burlap, which is dragged "behind a paver". In transverse drag, the carpet broom or burlap is manually dragged across the plastic concrete pavement surface. When burlap is dragged instead of a turf, the surface formed is called a burlap drag or hessian drag, the term hessian being an archaic reference to fabric**.** The typical dimensions of drag textures are generally in the range of 0.5 to 2 mm.

Unlike the turf drag tining of a finished surface is achieved by dragging a rake across the finished surface (transverse tine) or along the finished surface (longitudinal tine). Illustration of texturing of fresh concrete is shown in FIGURE 2.1. The tining process uses typical rakes that have prongs 1 mm thick at 19 mm intervals set up to create the texture without unduly moving the aggregate at the surface.

Inverted Turf Dragging

Drag Surface Texture

Raking / Tining

Tining Texture

FIGURE 2.1: Fresh Concrete Texturing

2.2.3: Textures Established in Semi Hardened Concrete: Exposed Aggregate Texturing

Very few texture types are established in the semi-hardened concrete state because of chemical and physical changes (hydration reaction) that are still occurring at that time. The exposed aggregate texture is the quintessence of semi-hardened concrete texturing. The creation of an exposed aggregate surface actually begins with a suitable mix design involving a well-graded or single-graded aggregate gradation [2.1].

Retarder Application Process

Surface Brushing

Resulting Surface

FIGURE 2.2 Method of Creating Textures in Semi Hardened State: Exposed Aggregate Texturing

The construction process used is conventional, but immediately after finishing, a set-retarding admixture is applied to the surface. The engineer monitors the surface hourly to determine when the concrete is semi-hardened enough to allow paste removal while the aggregates are undisturbed. Paste removal is done either by brushing in order to create the exposed aggregate finish (see FIGURE 2.2 for an illustration of the process leading to the exposed aggregate finish) or by power-washing.

2.2.4: Textures Established in Hardened Concrete

There is a good number of texture types established in hardened concrete but the only one relevant to this study is the diamond ground textures. Diamond grinding is occasionally performed either as a first texturing after the finished concrete is hardened or as rehabilitation of an existing pavement/texture after many years of service. Diamond grinding involves the use of very large equipment with large rotating parts equipped with cutting disks that are stacked on a shaft which is controlled to impart certain required configurations on the pavement surface by cutting. (See FIGURE 2.3.) The surface produced by diamond grinding is anisotropic and mainly longitudinal. In diamond grinding, the spacers and diamond tipped cutters/blades can be stacked differently to achieve different geometric configurations with the same equipment. Different stacking arrangements have resulted in versions of the diamond grind known as the traditional grind characterized by moderate groove intervals, the innovative grind characterized by larger groove intervals and the ultimate grind which is a more recent version of the innovative grind achieved by first performing a flush (non-configured) grind of the surface before the innovative grinding. These differences will be shown to be important when the grinding configurations are discussed later.

Diamond Grinding Process and Surface Created

Diamond Ground Surface

FIGURE 2.3: Textures Established in Hardened State: Diamond Grinding

2.3: FEATURES OF PAVEMENT SURFACES

2.3.1: Microtexture and Megatexture

After introducing various texture types, it is now expedient to identify and discuss certain geometric characteristics of pavement surfaces. Surface geometric features in the order of 0 mm to 50 mm are within the microtexture and macrotexture range. Features between 50 mm and 5000 mm range are mega texture or giga texture or pavement roughness features. As implied pavement surface characteristics in this range affect pavement roughness and in consequence, ride quality [2.2] [2.3]. These texture dimension groups being different by orders of magnitude affect surface characteristics (including noise) through different mechanisms.

In this discussion it is important to note that the overarching goal of this thesis is to develop a phenomenological model for noise prediction. While various texture types may exhibit different values of identified geometric variables, the geometric variables also to be examined inconsideration of possible input to a phenomenological tire pavement noise prediction model.

2.3.2: Characterizing Smaller Scale Pavement Surface Features

Spatial properties in the micro texture and macrotexture dimensions are described by asperity interval (ASP), texture depth (MPD), and the probability density function of the texture height ("spikiness" SP). These features are briefly described below. In addition, due to the importance of determining tire pavement interactions and hence noise, the attribute of texture direction (DIR) is also discussed.

Asperity Interval (ASP)

The asperity interval is the average interval of repeating patterns of asperity in a pavement texture. It is determined by measuring a large number of asperities over a known distance and dividing the distance by the number of asperities encountered in that line. The asperity interval of a pavement surface determines to a large extent how the tire features envelops the asperities [2.5], [2.6] and how frequently tread block impact may occur.

The asperity interval ranges from 2 mm in drag textures to 18 mm in certain tined textures. Certain characteristic configurations are evident in most textures [2.2]. FIGURE 2.4 is a magnification of a section taken through a turf drag texture.

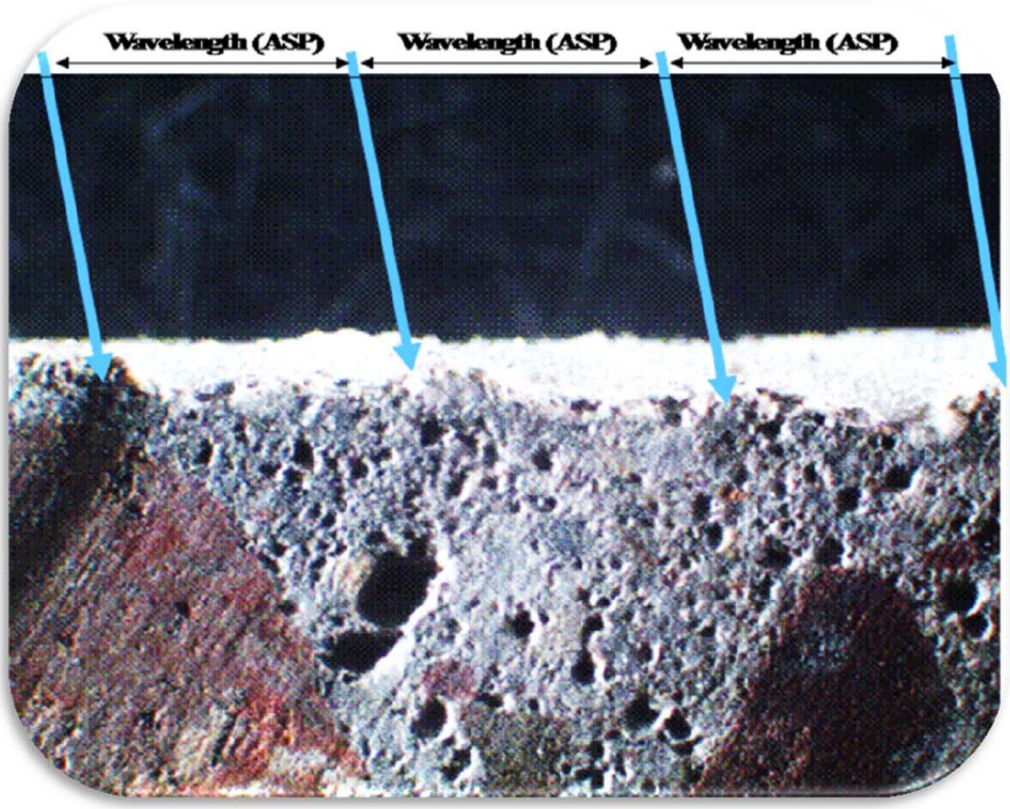

FIGURE 2.4: Magnified (X100) Cross Section through a Drag Texture Indicating Definite Configuration Patterns. The patterns are vivid in other texture types.

Mean Profile depth (MPD)

The texture depth, characterized as the mean profile depth (MPD) [2.4], is the average depth of texture in a textured surface. This property is measured using a circular track meter (CTM ASTM E-2157). This instrument is equipped with a charged coupled device (CCD) laser displacement sensor that sweeps on the pavement surface a circle 11.2 in (284 mm) diameter or 35 in (892 mm) circumference. The displacement sensor for this instrument is mounted on an arm that rotates at 3 inches (76 mm) above the surface. The arm moves at a tangential velocity of 6 m/min. From the mounting, CCD is sampled 1,024 times per revolution providing a sample spacing of 0.87 mm. The data is segmented into eight 111.5 mm arcs of 128 samples each. From each segment, the computer software computes the mean profile depth (MPD). MPD values are typically

from 0.2 mm in drag textures to 2.4 mm in certain ground textures and most tined textures.

Spikiness (SP)

The spikiness (SP) is considered to be an important parameter in determining tire pavement noise because it is an indication of the shape function of the asperities in terms of the frequency distribution of spiked outcrops or sharp valleys. It requires a careful definition as to what it is and how it is measured.

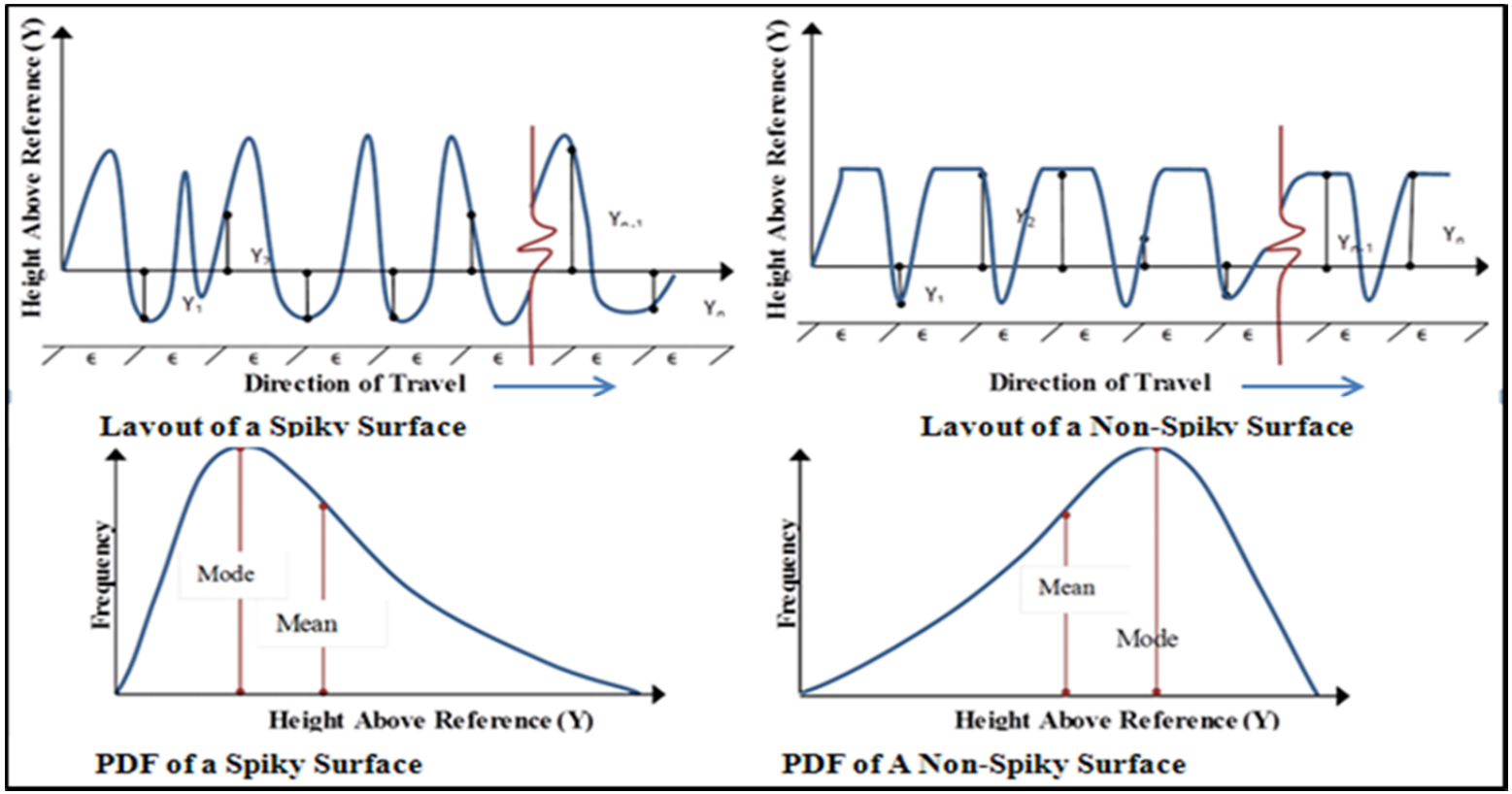

FIGURE 2.5: Layout and Probability Density Function of Spiky and Non-Spiky Textures

Consider an ideal pavement texture profile aligned in a certain direction of travel. The top frames in FIGURE 2.5 show two potential profiles. The associated probability density function (pdf) [2.7], [2.8] of surface height for each of these examples is plotted below each profile. In the left hand plot, the pdf shows a skew to the right (the mean > mode) indicating that the profile exhibits sharp positive peaks. A surface with this type of profile is said to have a positive spikiness. By contrast, in the right hand profile, the mean of the pdf is less than its mode indicating that the profile has sharp valleys. A surface with this type of profile is said to have a negative spikiness.

In real systems the profile is obtained by height Y_1 measurements at equal small steps "ε" along the ordinate direction, (see FIGURE 2.5). The spikiness value is then obtained from a discrete comparison of the mean to the mode of the texture height distribution function resulting in the following equation

$$\mathrm{SKU} = \frac{\sum_{i=1}^{N}(Y_i - \bar{Y})^3}{(N-1)s^3} \tag{2.1}$$

where

SKU is skewness,

$\bar{Y}$ is mean height,

N is the number of measurements, and

S is standard deviation. Then the spikiness, a categorical variable, defined as

$$\mathrm{SP} = \begin{cases} 1, & \mathrm{SKU} > 0 \\ 0, & \mathrm{SKU} \leq 0 \end{cases} \tag{2.2}$$

Note that the accuracy of (2.1) depends on ensuring that $\varepsilon \ll |\bar{Y}|$ for non-zero $|\bar{Y}|$.

Details of spikiness quantification are elucidated in the development of a phenomenological model [2.9]

Texture Direction (DIR)

In addition to the features above, the prominent direction of texturing (DIR), whether transverse or longitudinal, also characterizes the pavement surface. Transverse texture asperities impact the tire with a frequency and pattern that is different from longitudinal textures. In the former, asperities are aligned across the direction of tire pavement interaction, but in the latter, the prominent tire and texture asperities are collinear. The direction of texturing thus governs tire surface interaction mechanisms including the frequency of tire tread block impact and the ease of tire texture air compression relief. As a result, the tonal content of the tire pavement noise on transverse textures is associated with whining noise at most practical texture intervals of 16 mm to 25mm. In a similar manner to spikiness the direction, DIR is also a categorical variable set as DIR=0 for longitudinal direction; DIR =1 for transverse direction. The assignment of DIR=0 recognizes the fact that longitudinal textures probably are quieter than transverse textures. A summary of the various measures of surface texture is shown in TABLE 2.1.

TABLE 2.1: Starting Variables

VARIABLE	DEFINITION / DESCRIPTION
IRI	International Roughness Index, m/km measured with a laser equipped accelerometer (profiler) and not filtered
SP	Texture Orientation / Spikiness. The texture is of positive orientation (spiky) if the riding surface is below the asperities and negative when the asperities are indented (SP =0)
MPD	Mean Profile Depth (mm). In a ground texture, obtained from the use of a circular track meter ASTM E-2157.
DIR	Direction of texture. Categorical variable in which 0 is assigned to longitudinal texture and 1 is assigned to transverse texture.
ASPGW	Asperity groove width (mm) mean interval between repeating texture patterns
T	Air temperature at the time of noise measurement (^{0} K).

2.3.3: Characterizing Larger Scale Pavement Surface Features

As noted above, large scale surface features occur on the scale of 0.5 - 50 meters wavelengths. Examples are warp and curl of the pavement section. In addition to causing noise (see discussion in Chapter 3), such features are the overriding control on the pavement ride quality. Hence measuring the ride quality is a proxy for measuring the nature of large scale pavement features.

The International Roughness Index (IRI) is the roughness index most commonly obtained from measuring longitudinal road profiles. It is calculated using a quarter-car vehicle mathematical model, whose response is accumulated to yield a roughness index value with units of slope (in/mi, m/km, etc.) [2.10]. Originally, it was determined with systems equipped with suspension known as the "quarter car", but currently, the profile can be determined by various devices including dipsticks, lightweight profilers, and high speed

profilers. The profile measured is, in any case, subjected to the quarter-car algorithm for the computation of IRI. This index is correlated to curling and warping of pavements [2.11], faulting, [2.12], and various pavement distress conditions [2.13].

2.4: MEASUREMENT OF TEXTURE PARAMETERS

2.4.1 Measurement of Small Scale Features

Some pavement surface texture geometric features are measured using a circular track meter (CTM) ASTM E 2157 (see FIGURE 2.6). This device uses laser technology to obtain a digital elevation profile around the circumference of an 11 inch diameter circle on the pavement surface. From this data a mean profile depth (MPD) is obtained. On the other hand, the asperity interval (ASP) is obtained by breaking the circle into eight arcs and only considering the two arcs that are normal to the texture direction. Likewise, the profiles from these arc segments are also used in the determination of the spikiness SP (see FIGURE 2.5).

A texture measurement campaign was performed on different texture surface types in the MnROAD research facility from 2007 to 2010. This involved use of the CTM to measure texture on designated spots and at frequent intervals on the left wheel path and right wheel path of the concrete sections. The pavement sections tested included examples of each one of the texture types outlined at the beginning of this Chapter, viz: transverse tine, conventional diamond grind, innovative diamond grind, ultimate diamond grind, exposed aggregate and drag. This resulted in the data of TABLE 2.2, which identifies in terms of the key small scale features eight different pavement surface configurations.

FIGURE 2.6: Circular Track Meter ASTM E-2157 (ASP and SP)

TABLE 2.2: Different Texture Configurations and Measured Geometric Variables

TEXTURE TYPE	CONFIG #	ASP (mm)	ASPGW (mm)	DIR	SP	MPD (mm)
Transverse Tine	1a	15	6	1	0	0.81
	1b	18	6	1	0	0.85
Traditional Grind	2	6	3	0	1	0.91
Innovative Grind	3	15	3	0	0	1.21
Ultimate Grind	3*	16	3	0	0	1.19
Exposed Aggregates	4	9	9	1	1	0.7
Broom/Turf Drag	5a	3	2	0	1	0.39
	5b	3	2	1	1	0.34

2.4.2: Measurement of Large Scale Texture Properties

The IRI, which as noted above as a proxy for large scale texture features, were measured with a light weight profiler (FIGURE 2.7). The equipment consists of an accelerometer that emits a laser beam so that when the equipment is driven through a test section the vertical acceleration of a quarter-car due to the profile is recorded as a profilogram (see FIGURE 2.8). From this profilogram, the single measured IRI is obtained as the summation of the absolute deviation—relative to an assumed mean—per unit length of travel (i.e., inches per mile). Seasonal measurements were conducted on all the sections analyzed. In each round of testing, 3 runs were performed in each lane and the results were recorded for each section.

An example of the IRI data obtained in one of the sections is shown in FIGURE 2.8 and IRI values for a particular section are given in TABLE 2.3.

FIGURE 2.7: Lightweight Profiler

TABLE 2.3: Example of IRI Summary for a Section Measured 8/9/07

RUN #	IRI (in/mi)
1	83.3
2	68.0
3	72.8
4	78.5

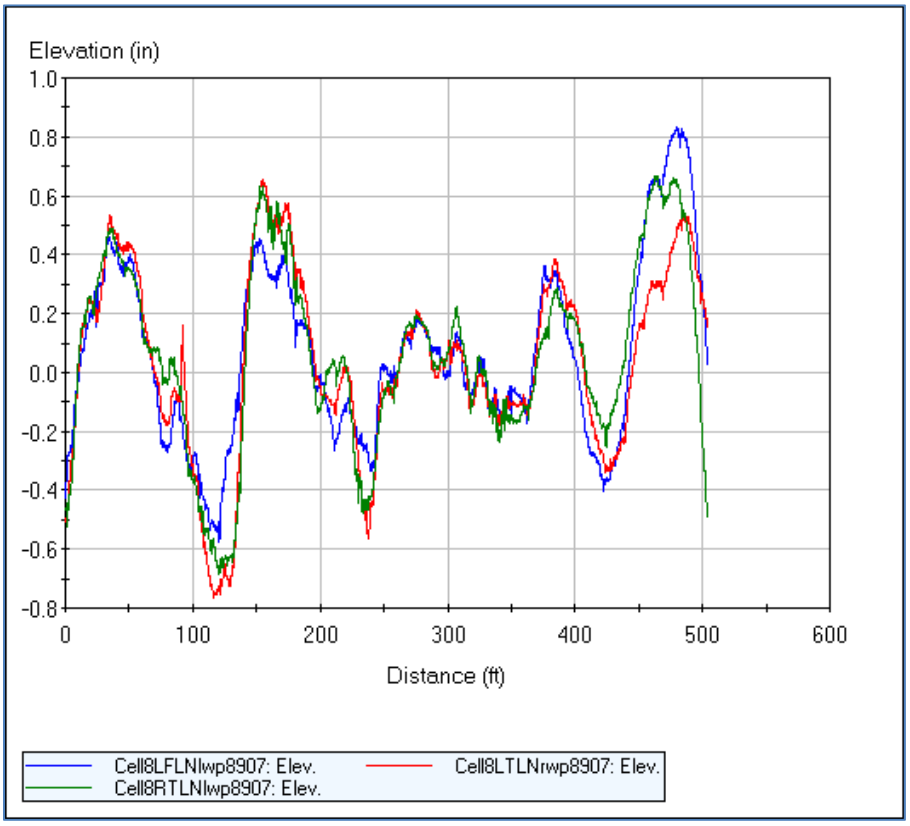

FIGURE 2.8: Example of Profilogram from a Test Section.

2.5: STANDARD REFERENCE TEST TIRE

It is expedient to introduce and discuss some properties of the standard reference test tire (SRTT) because it is the standard tire utilized in this research. SRTT (ASTM E-2943) is not necessarily a quiet tire, but one with standard dimensions of tire groove width, groove depth and tread block patterns shown in FIGURE 2.9. To normalize pavement surface

variables, corresponding tire dimensions were introduced. The pavement texture variables were divided by corresponding tire variables to achieve dimensionless variables for the proposed model. From figure 2.9 it can be seen that the SRTT is basically longitudinally tined. The SRTT is characterized by tread blocks with dimples, longitudinal grooves and less prominent transverse air relief features. The dimensions of relevance to this study particularly in the normalization of corresponding pavement configurations include: tire groove depth, (GDT); asperity interval of tire (ASPT) and asperity groove width of tire, (ASPGWT).These variables were used in normalizing the pavement texture configurations. This leads to the variable $\frac{\text{ASP}}{\text{ASPT}}$ while an alternative approach considers another variable, $\frac{\text{ASPGW}}{\text{ASPGWT}}$ where:

ASP is asperity interval of the surface texture and
ASPGW is the asperity groove width of the surface texture

The influence of the tire alone obtains with an untextured surface, but more air pressure relief occurs with a textured surface. More tread block impact is expected to occur in textures with a larger tread block interval and vice versa.

Measuring Tire Groove depth

Measuring Tire Groove Width

Measuring Tire Tread Block

Pavement Surface Configurations

FIGURE 2.9: Dimensions of the SRTT (ASTM E2493) Used in the Experiment

2.6: CHAPTER SUMMARY

Textures are created in the fresh concrete, semi-hardened concrete and hardened concrete states. Although different texturing methods confer different geometries to the surface, it is hypothesized that the geometries and not the texturing methods account for the surface properties. Going forward with this hypothesis, length and depth scales of asperity interval and mean profile depth properties respectively have been defined. A two-dimensional property (the spikiness) (SP) has been discussed. Its significance is evident

as a descriptor of the texture orientation indicating how upwardly spiked or not the configuration is. The direction (DIR) of texturing was introduced as a major feature that affects how the tire asperities may interact with the pavement surface collinearly (longitudinal textures) or orthogonally (transverse textures). The international roughness index serves as proxy for some surface features in the realm of mega texture and giga texture.

CHAPTER 3: THE TIRE PAVEMENT NOISE MODEL

3.1 CHAPTER INTRODUCTION

Tire-pavement interaction noise is affected by many factors such as the pavement surface characteristics (discussed in the previous chapter), tire characteristics, vehicle speed, pavement conditions and the ambient environment. The objective of this chapter is to establish a basic form for a model that can be used to predict tire-pavement interaction noise. Two major components of this model are proposed:

- Intrinsic Tire Noise (ITN): The noise associated with a tire running on a smooth untextured pavement and
- Noise related to pavement geometries.

This second component can in turn be separated into two classes:

- Noise associated with large scale construction features such as the warp, curl and joint intervals of the concrete pavement sections, as well as
- Noise associated with the smaller scale surface finish features.

In the remainder of this chapter each of these noise generating features will be investigated with the objective of building a general form for a tire-pavement noise model.

3.2: WHAT IS NOISE?

Noise is understood as “undesirable sound” according to differing perception and interest of the recipient [1.7] [3.1]. Sound is made up of pressure waves generated by a vibrating source and then transmitted through a solid, liquid, or gas; a given sound wave is characterized by frequency and amplitude. At a point away from the source, the sound intensity (defined as the power per unit area) of a given sound wave at a given frequency is defined as

$$SI = p * v \tag{3.1}$$

where

p, referred to as sound pressure, is the root mean of the pressure variations at the point in question, and

v is the velocity of the sound wave (which is not the speed of sound).

From this definition the sound intensity level SIL, measured in decibels dB, is defined in as:

$$SIL = 10\ \mathrm{Log}\left(\frac{SI}{SI_o}\right) \tag{3.2}$$

where

$SI_0 = 10^{-12}$ Watts/m^2;

SI is sound intensity (watts/m2)

SIL is sound intensity level in decibel (dB).

This chosen background reference sound intensity ($SI_0 = 10^{-12}$ Watts/m^2) is the quietest sound a typical young human with undamaged hearing can detect at 1,000 Hz. [1.7]. Using this background reference SIL unit is sometimes referred to as dBA since scale associated with the reference is called the "A" weighted scale. The value of SIL decreases with the inverse square of the distance from the source. In the vicinity of the source typical values span from 190 dB at a distance of 1000 feet for a jet engine to the quiet whisper of 30 dB which is the background noise in a library.

As noted in Chapter 1, at speeds in excess of 30 mph the dominant contribution to traffic noise is the tire pavement interactions. In assessing this noise it is important to account for both the distance from the source and the range of frequencies of the waves that

contribute to the noise. The American Association of State Highway and Transportation Officials (AASHTO) Interim Standard for measuring this noise is defined as On Board Sound Intensity, (OBSI) [3.2]. This value is measured at a diagonal distance of 5 inches from the contact patch between a standard test tire and the pavement on a vehicle travelling at 96 km/h. The OBSI is made up of a combination of the sound intensities levels measured over 12 frequencies in the one-third octave band, i.e., the frequencies

$$f = 400 * 2^{\left(\frac{i-1}{3}\right)} \quad \text{for } i = 1,2,..12 \tag{3.3}$$

where

f is frequency (Hertz) where 400 is the lowest

"i" is serial number of the frequency value from 1 to 12

Each individual sound intensity level SIL_i measured at the specified frequency is then combined into the OBSI via the following equation:

$$OBSI = 10 \log_{10}\left[10^{\left(\frac{SIL_1}{10}\right)} + 10^{\left(\frac{SIL_2}{10}\right)} + \cdots + 10^{\left(\frac{SIL_{12}}{10}\right)} \right] \tag{3.4}$$

3.3: THE PROPOSED MODEL FORM

A full discussion on field measurement of OBSI for a variety of pavements types and conditions is covered in the next chapter. The current objective is to propose a theoretical model that can be used to analyze this field data. In arriving at the model form for OBSI it is recognized that the major contributor will be the intrinsic tire noise (ITN). Additional contributions from the tire pavement interactions with large scale features (TPI^+) and small scale features (TPI^-), which are well within the hearing detection of humans, are much smaller. As such we assume that the TPI contributions can be included in a model via a simple addition. Thus the starting form for the proposed model is

$$OBSI = ITN + TPI^{+} + TPI^{-} \quad (3.5)$$

The expanded form of each of these terms is discussed in detail below.

3.4: INTRINSIC TIRE NOISE

Intrinsic Tire Noise (ITN) is caused by tire vibration and air compression relief in the standard tire on a smooth pavement. Considering the body of knowledge of sound intensity and environmental effects, theories [3.3], [3.4] suggest that the ITN will scale proportion to density and speed of sound in the form:

$$ITN \sim \rho c \quad (3.6)$$

where

ρ is the air density and

c is the speed of sound.

Under traffic conditions both of these quantities are principally controlled by the ambient temperature (T). In particular, for a temperature in the range T=250 to 310 K, the speed of sound in air can be approximated by the linear relationship [3.3]

$$c = 167 + 0.6T \quad (3.7)$$

where

T is air temperature (Kelvin)

Further, the density of air can be related to the temperature through the ideal gas equation

$$\rho = \frac{P}{RT} \quad (3.8)$$

where

P is the atmospheric pressure (assumed to be the constant value of ~10^5 Pa in this work) and R is the gas constant (8.3 J/K).

Thus

$$ITN = \frac{A^*}{T} + B^* \tag{3.9}$$

where

A^* and B^* are constants.

A*= (A-B) and

B*=293B

Thus Equation 3.9 can be written in the more convenient form based on European Union reference standard for temperature effect on sound intensity[3.5]:

$$\mathrm{ITN} = \mathrm{A} + \frac{293 - \mathrm{T}}{\mathrm{T}} \tag{3.10}$$

This equation clearly shows the relationship between ITN and temperature and provides a base value of the intrinsic tire noise, the constant A, at a reference temperature of T = 293°K.

3.5: TIRE PAVEMENT NOISE

3.5.1: Scales of Texture

As noted in the introduction and Chapter 2, the geometric features of the pavement will also contribute to the overall OBSI by adding on to the ITN. These Tire Pavement

Interaction (TPI) noise contributions can be split into two classes: OBSI contributions due to large scale pavement features associated with construction denoted as TPI+ and contributions due to surface finish denoted by TPI^-. Each of these classes generates its own sub-model for use in (3.5).

3.5.2: Larger Scale Texture Effects:

Certain geometric features in the pavement occur as a result of design, construction and/or deterioration. These features, typically with length scales ≥ 0.16 m, include joint interval, joint width, warp and curl. The vehicle tires interact with these geometric features and through the occurrence of response phenomena known as body bounce, axle hop and joint slap, noise is generated. Body bounce is the low frequency resonance of the vehicle while axle hop is the higher frequency resonance of the tire and axle. By contrast joint slap is simply the noise generated as the tire encounters geometric differences across the joint opening. It is noted that all of these large scale features will also influence the ride quality expressed through the International Roughness Index (IRI) (see discussion in Chapter 2). Hence the hypothesis made here is that the IRI is a proxy for the sound intensity from the large scale pavement features (TPI+), i.e.

$$TPI^+ = C*IRI \tag{3.11}$$

Typical IRI values are in the range between 0.05 m/km for a very smooth road to 15 m/km in a road where all panels are faulted to 1 inch and warped to 1 inch. Here we chose a reference value (IRIT) of 15 m/km to normalize the equation.

$$TPI^+ = C * \frac{IRI}{IRIT} \tag{3.12}$$

3.5.3: Smaller Scale Texture

As vehicular tires interact with surface textures certain distinct mechanisms occur. These include tread block impact, air compression relief and other miscellaneous mechanisms (see Figure 3.1). These mechanisms represent the actual types of sound generated and, when understood, may facilitate the development of a quieter pavement. The two leading noise causes are

(i) Tread block impact and

(ii) Air compression relief (see Figure 3.1).

In the former, as the tire rolls along, the tire tread blocks impact the pavement surface texture, essentially imitating the continuous impact of a small mallet on the surface texture [1.6] [1.7]. In the latter compression of air in the pavement texture takes place at the leading edge of the contact patch. The subsequent relief of this compression results in noise. The relief mechanism is dictated by the texture type [1.7]. For instance, air compression relief in transverse textures is intermittent, while in longitudinal textures the relief occurs smoothly.

There are three levels of pavement texture variables that may be important in determining tire pavement interaction noise. The first is a measure of the geometry of the asperities in the plan-form determined by the distance between asperities, ASP, or the width of the asperity groove, ASPGW. The second is the mean profile depth, MPD. The third is the so called spikiness - a measure of the profile texture distribution, defined in Chapter 2. This latter variable takes two values: SP=0 when the texture is negative (deep narrow valley below a mean flat surface) or SP=1 when the texture is positive (sharp peaks above a mean flat surface). Each of these effects on tire pavement noise is discussed below.

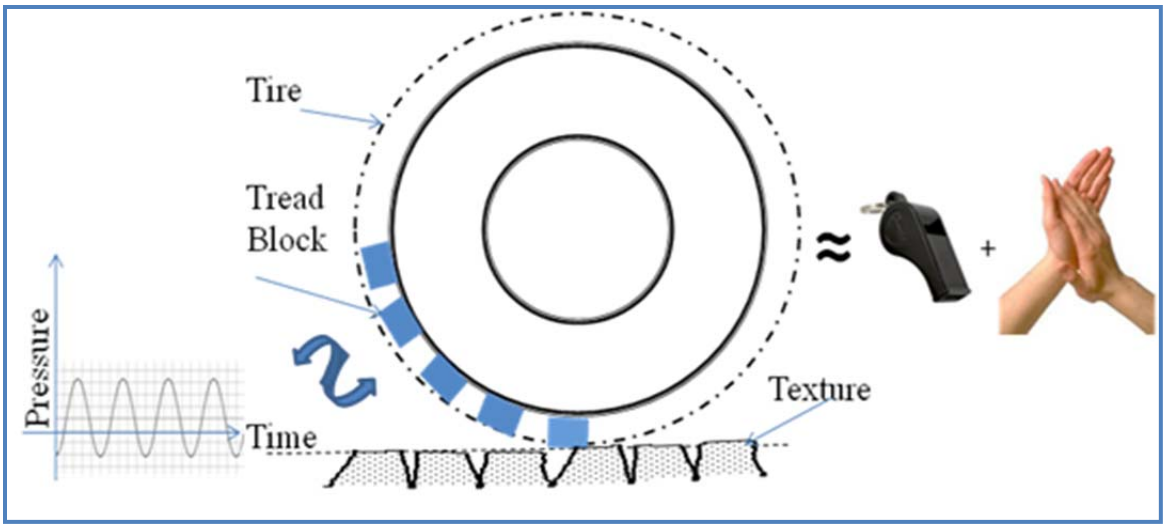

Air Compression Relief Mechanism

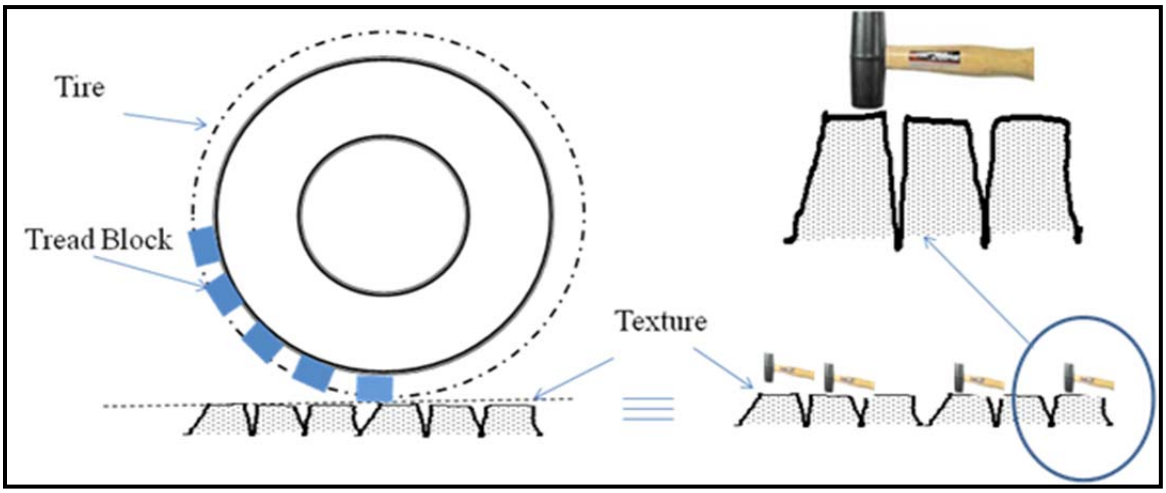

Tire Tread block Impact Mechanism

FIGURE 3.1: Major Tire Texture Noise Mechanisms: Tire Pavement Tread Block and Air-Compression Noise

(i) Plan-form

The plan-form texture can be measured in terms of the ASP or ASPGW. Closely spaced asperities (ASP→0) or smaller groove width (ASPGW→0) may ordinarily increase frequency of tread block impact implying more noise. In cases where there is larger

asperity interval (ASP→∞) or more groove width (ASPGW→∞) there is lesser asperity intervention and easier air pressure compression relief implying less noise. Thus these impacts of plan-form can be included in the model with terms of the form ASPT/ASP or ASPGWT/ASPGW, where ASPT and ASPGWT normalization terms are the asperity spacing and asperity groove width of the test tire (ASPT= 25 mm and ASPGWT= 9 mm). In this way the first term in the equation for the contribution from small scale features has two alternative forms:

$$\mathrm{TPI}^{-} = \mathrm{E}\left(\frac{\mathrm{ASPT}}{\mathrm{ASP}}\right) \tag{3.13a}$$

Alternatively,

$$\mathrm{TPI}^{-} = \breve{\mathrm{E}}\left(\frac{\mathrm{ASPGWT}}{\mathrm{ASPGW}}\right) \tag{3.13b}$$

where

E is the model constant for normalized asperity interval and

$\breve{\mathrm{E}}$ Is the model constant for normalized asperity groove width.

(ii) Groove Depth

It is difficult to hypothesize on the effect of mean profile depth based on conflicting opinions in the industry, but larger mean profile depth may imply lesser noise. However, Hamet and Klein [3.6] postulate, that since actual tire textures bridge asperities but do not envelop the entire texture depth, mean profile depth may not be a good predictor of tire pavement noise. Nevertheless, an attempt will be made to evaluate the impact of this variable by adding a term of the form GDT/MPD to the OBSI model, where GDT is the average groove depth of the tire (8 mm) hence this normalized MPD term is added equations 3.13 a and 3.13b:

$$\mathrm{TPI}^{-} = \mathrm{E}\left(\frac{\mathrm{ASPT}}{\mathrm{ASP}}\right) + \mathrm{G}\left(\frac{\mathrm{GDT}}{\mathrm{MPD}}\right) \quad (3.14a)$$

Alternatively,

$$\mathrm{TPI}^{-} = \breve{\mathrm{E}}\left(\frac{\mathrm{ASGWT}}{\mathrm{ASPGW}}\right) + \breve{\mathrm{G}}\left(\frac{\mathrm{GDT}}{\mathrm{MPD}}\right) \quad (3.14b)$$

where

G is the model constant for normalized asperity interval and

$\breve{\mathrm{G}}$ Is the model constant for normalized mean profile depth in alternate model.

(iii) Surface Texture Spikiness

As discussed in Chapter 2, an important property of a pavement texturing is its so-called spikiness. In essence, spikiness can be classified as positive sharp peaks separated by flat valleys or negative mesa like high points separated by sharp valleys (see Figure 2.5). It is hypothesized that positive textured pavements (SP=1) are noisier than negatively textured pavements (SP=0). This is because a positive texture would incur a significantly larger number of tread-block impacts per unit distance of travel. Furthermore, a negative texture (SP=0) may act as an inefficient (leaking) horn, thus reducing the horn effect, while a positive texture (SP=1) may present a horn with multiple channels. In addition, spikiness of texture may affect slip-snap and stick-snap noise generation mechanism. Slip-snap and stick-snap are associated with hysteretic phenomena [3.7] and with the characteristics of rubber friction. A rolling tire experiences localized instantaneous collapse at the contact patch, but this interfacial contact is released more rapidly than the tire would allow, thus causing negative pressures and suction. Therefore adding the normalized spikiness term, the expression for small scale texture related noise becomes:

$$\mathrm{TPI}^{-} = E\left(\frac{\mathrm{ASPT}}{\mathrm{ASP}}\right) + G\left(\frac{\mathrm{GDT}}{\mathrm{MPD}}\right) + \mathrm{J(SP)} \quad (3.15a)$$

Alternatively,

$$\mathrm{TPI}^{-} = \check{E}\left(\frac{\mathrm{ASGWT}}{\mathrm{ASPGW}}\right) + \check{G}\left(\frac{\mathrm{GDT}}{\mathrm{MPD}}\right) + \check{\mathrm{J}}(\mathrm{SP}) \qquad (3.15b)$$

where

J is the model constant for spikiness and

$\check{\mathrm{J}}$ Is the model constant for spikiness in the alternative model-form.

(iv) Direction

The texture on the pavement can be aligned with the direction of travel DIR=0 or transverse to the direction of travel DIR=1. Due to the ability for better pressure relief, it is expected that texture aligned with the traffic direction will be quieter. In particular it is noted that transverse asperities cause increased tread block impact. The concatenations result in a whining sound when the asperities are encountered at the resonant frequency of the standard reference test tire (1000 Hz). For instance, at a speed of 60 miles per hour, a moving tire encountering a one-inch ASP with transverse texture results in a 1000 Hz frequency, causing a loud whine.

In the light of the above, two alternative candidate models for the contribution of surface finish to OBSI are proposed: a model that uses ASP as the plan-form measure is of the form:

$$\mathrm{TP\,I}^{-} = \left[\left(\frac{\mathrm{ASPT}}{\mathrm{ASP}}\right)(\mathrm{D} * \mathrm{DIR} + \mathrm{E})\right] + \left[\left(\frac{\mathrm{TD}}{\mathrm{MPD}}\right)(\mathrm{F} * \mathrm{DIR} + \mathrm{G})\right]$$

$$+[(SP)(\mathrm{J} * \mathrm{DIR} + \mathrm{K})] \qquad (3.16a)$$

The alternative model that uses ASPGW as a plan-form measure is of the form:

$$\mathrm{TPI}^{-} = \left[\left(\frac{\mathrm{ASPGWT}}{\mathrm{ASPGW}}\right)(\mathrm{D} * \mathrm{DIR} + \mathrm{E})\right] + \left[\left(\frac{\mathrm{TD}}{\mathrm{MPD}}\right)(\mathrm{F} * \mathrm{DIR} + \mathrm{G})\right] +$$

$$[(SP)(\mathrm{J} * \mathrm{DIR} + \mathrm{K})] \qquad (3.16b)$$

Note that these models are arranged so that the constants will take positive values. This way the effect of DIR is clearly seen. It is when this variable is DIR=1 (texture normal to travel direction) that the contribution to noise from the various texture terms should be increased.

3.6: THE FINAL MODEL FORM

Combining Equations 3.10, 3.12 and 3.16, two final model forms are derived as:

$$\mathrm{OBSI} = \mathrm{A} + \mathrm{B}\left(\frac{293-\mathrm{T}}{\mathrm{T}}\right) + \mathrm{C}\left(\frac{\mathrm{IRI}}{\mathrm{IRIT}}\right) + \mathrm{D}\left[\left(\frac{\mathrm{ASPT}}{\mathrm{ASP}}\right)(\mathrm{D} * \mathrm{DIR} + \mathrm{E})\right] + \left[\left(\frac{\mathrm{TD}}{\mathrm{MPD}}\right)(\mathrm{F} * \mathrm{DIR} + \mathrm{G})\right] + [(\mathrm{SP})(\mathrm{J} * \mathrm{DIR} + \mathrm{K})] \qquad (3.17a)$$

Alternatively,

$$\mathrm{OBSI} = \mathrm{A} + \mathrm{B}\left(\frac{293-\mathrm{T}}{\mathrm{T}}\right) + \mathrm{C}\left(\frac{\mathrm{IRI}}{\mathrm{IRIT}}\right) + \mathrm{D}\left[\left(\frac{\mathrm{ASPGWT}}{\mathrm{ASPGW}}\right)(\mathrm{D} * \mathrm{DIR} + \mathrm{E})\right] + \left[\left(\frac{\mathrm{TD}}{\mathrm{MPD}}\right)(\mathrm{F} * \mathrm{DIR} + \mathrm{G})\right] + [(\mathrm{SP})(\mathrm{J} * \mathrm{DIR} + \mathrm{K})] \qquad (3.17b)$$

where

A, B,C,D, E,F, G, J and K are the model constants in the two alternatives model-forms

In all further analysis the normalized forms of these equations may be used, i.e.,

$$OBSI = A + BT^* + C\,IRI^* + [(ASP^*)(D\,x\,DIR\ + E)] + [(MPD^*)(F\,x\,DIR\ + G)] + [(SP)(J\,x\,DIR\ + K)] \quad (3.18a)$$

Alternatively,

$$OBSI = A + BT^* + C\,IRI^* + [(ASPGW^*)(D\,x\,DIR\ + E)] + [(MPD^*)\,(F\,x\,DIR\ + G)] + [(SP)\,(J\,x\,DIR\ + K)] \quad (3.18b)$$

and

$$T^* = \frac{293 - T}{T} \quad (3.19)$$

Moreover,

$$IRI^* = \frac{IRI}{IRIT} \quad (3.20)$$

$$ASP^* = \frac{ASPT}{ASP} \quad (3.21)$$

$$ASPGW^* = \frac{ASPGWT}{ASPGW} \quad (3.22)$$

$$MPD * = \frac{GDT}{MPD} \quad (3.23)$$

where

IRIT is taken as 15 m/km (1000 inches/mile). This is the theoretical IRI for a surface of extremely poor ride quality that can be obtained if all panels are warped 1 inch at mid-slab and every joint in that pavement is faulted by 1 inch.

In this study, the asperity interval of tire , ASPT was assumed to be 25 mm and the asperity groove width ASPGWT was assumed to be 9 mm and the tire groove depth GDT was assumed to be 9.25 mm.

In addition, for notational convenience the * superscript, indicating normalized variables will be dropped. From this point forward, the task is to find out which one of Equation 3.18a or Equation 3.18b is the best form, which terms can be dropped, and appropriate values for the coefficients. This will be done in two steps. In the next chapter the results of an extensive measuring campaign for the noise of concrete pavements across a wide range of surface finishes and conditions is reported. A summary of starting variables is shown in Table 2.1. In the following chapter this data is used to statistically select an appropriate model form the candidate models in Equation 3.17.

3.7: CHAPTER SUMMARY

The model form of OBSI prediction is developed from 3 components of tire pavement noise which are intrinsic tire noise, small scale texture dimension source and large scale texture dimension sources. The suggested model-form consist of normalized variables structured such that conceived noisy features add to the overall while conceived quiet features reduce OBSI. Going forward, this model-form development will be validated by a large scale testing before actual prediction models can be produced. While the concept of spikiness may be have been briefly discussed in chapters 2 and 3, an elaborate discussion on this concept was made by Izevbekhai and Voller [3.8].

The next chapter discusses the measurement of noise and variables initially considered relevant to the prediction model.

CHAPTER 4: MEASUREMENT OF OBSI

4.1: CHAPTER INTRODUCTION

In Chapter 1, the dominance of tire pavement noise among the traffic noises in roadway speeds above the transitional speed was mentioned. Chapter 2 discussed the various texture types and their geometric properties, subsequently leading into Chapter 3 where the factors affecting tire pavement noise were identified and possible model forms for on board sound intensity (OBSI) were proposed. Before these models are investigated it is necessary to obtain reliable field measurements.

While there have been advancements and standardization of measurement of total traffic noise [1.3], insufficient attention has been paid to measurement of tire pavement noise. In effect, there is no existing standard for measurement of tire pavement interaction noise at the source [1.7]. The two main methods of traffic noise measurement commonly used in Europe and the United States are the statistical pass-by methods [1.3] and the close proximity (CPX) methods [1.6], [1.7]. The Federal (U.S.) standard for total traffic noise measurement (sound pressure) is the statistical pass-by (SPB) method [1.5]. In this method, microphones are stationed 25-ft or 50-ft from the roadway and consequently away from the source. Vehicle types, classification and speed are recorded along with measured noise [1.4] [4.3] to compute SPB value. The SPB thus measures overall noise but does not provide information on the tire pavement noise content. The need to characterize tire pavement noise led to the close-proximity (CPX) test method [1.7].

FIGURE 4.1: Left: Statistical Pass-By, Right: Close proximity (CPX) Method

The CPX method [4.1] uses a trailer that houses a standard reference test tire (SRTT) ASTM E2493 equipped with sound microphones in a housing that minimizes influx of air, wind effects and /or noise from other sources. In the CPX protocol, measurement is conducted at 40 miles-per-hour. The test method is widely acceptable but not suitable for isolation of all undesired noise sources in the spectral domain. Due to this limitation, the on-board-sound-intensity (OBSI) method was chosen as a more reliable method to characterize tire pavement noise. This method was used in this research and is now discussed in detail.

4.2: THE OBSI SET-UP AND USE IN THE TIRE PAVEMENT NOISE EXPERIMENT

The OBSI process is an interim American Association of State Highway and Transportation Officials (AASHTO) [4.2] [4.3] procedure in which measurement of the tire pavement noise is done with very sensitive microphones mounted a few inches from the tire pavement contact patch while the vehicle moves at 60 miles per hour. The process is generally categorized as a near-field measurement. In near-field measurements (distinguished from far-field measurement) the wavelength is much higher than the

distance from the noise source to the microphone. Additionally, the OBSI is designed to maximize as much as possible, measurement of the active portion of sound intensity. The active portion of the noise is actually emitted by the source and propagated away from the source. On the contrary, a source also emits a reactive component which is the result of another sound wave emitted by the source but traveling into the source. The reactive component has been variously explained by energy conversion [4.4] to forms other than sound [4.5] and mathematically as the complex component of the vectorial expression of the sound emission [4.6], [4.7] in the Helmholtz equation. The tire pavement contact patch is generally regarded as the source in this study.

OBSI in particular ensures that microphones are arranged very close to the contact patch and that by adequate windowing (Hamming Window) [4.6], only active emissions from the tire pavement patch are captured [4.7]. The OBSI device put together for this study consists of the following items:

- A dedicated sedan with power source
- Standard reference test tire (SRTT) ASTM E 2493
- Mainframe with 5 channel input
- Two rechargeable DC sources
- Dedicated computer
- Two paired phase-matched intensity microphones
- Rig system allowing rotation of tire and fixity of microphones cost made with security lug nuts and special attachments to the car frame.

The rear right hand side tire was removed and replaced with the standard reference test tire securing microphone to rig fixture. The test tire pressure was measured and ensured to be at 30 psi. The microphones were calibrated taking care to ensure that the four matched pairs of microphones and preamplifiers were plugged in to the front end unit, as well as 12 Volt power supply and ethernet (computer) cable. (See Figure 4.1a with more

details in Figures 4.2 and 4.3). In Figure 4.4, the schematic arrangement of the microphones with respect to the tire pavement contact patch is presented.

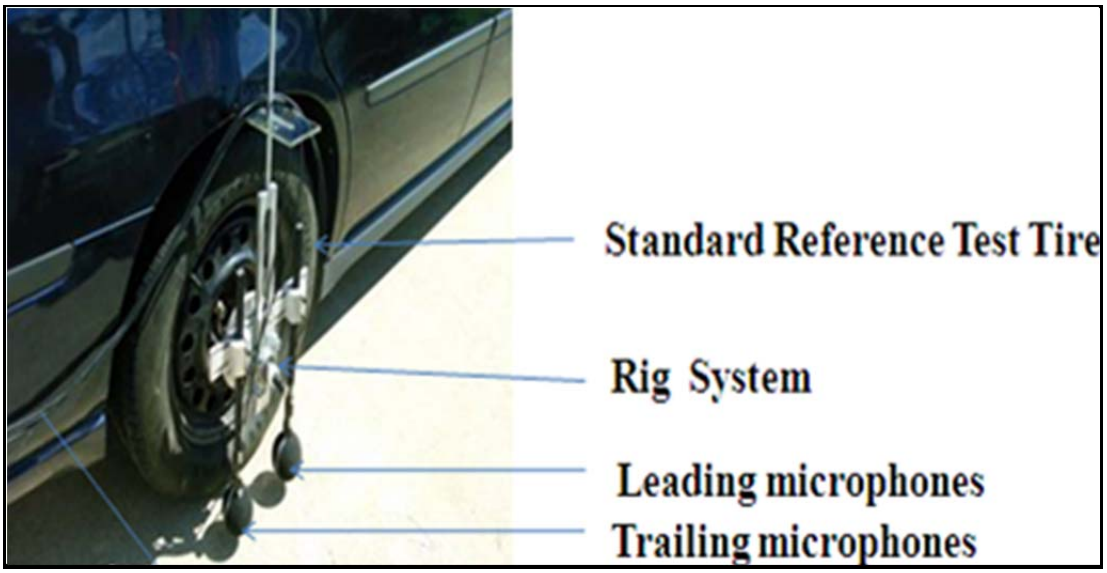

FIGURE 4.2: Layout (Set up of Experiment OBSI Test Tire, Rig and Communication Assembly)

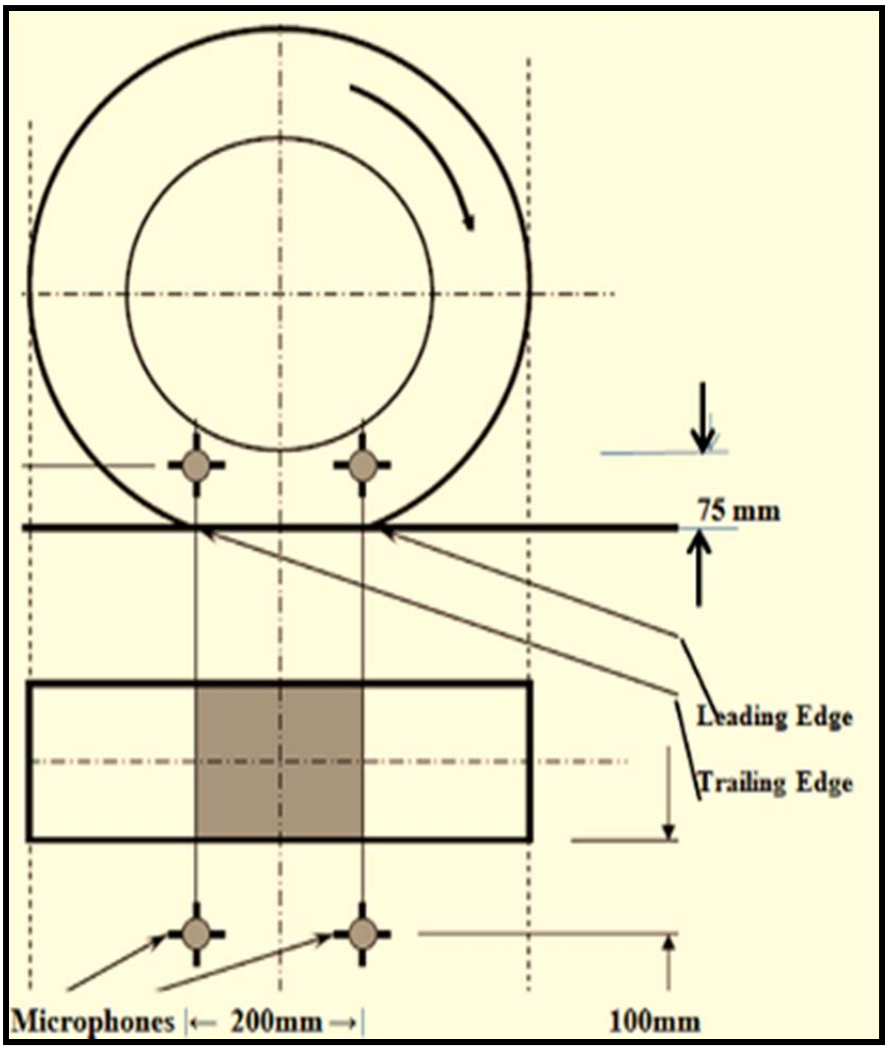

FIGURE 4.3: Layout of Microphones with Respect to Contact Patch
Top: Vertical View; Below: Plan

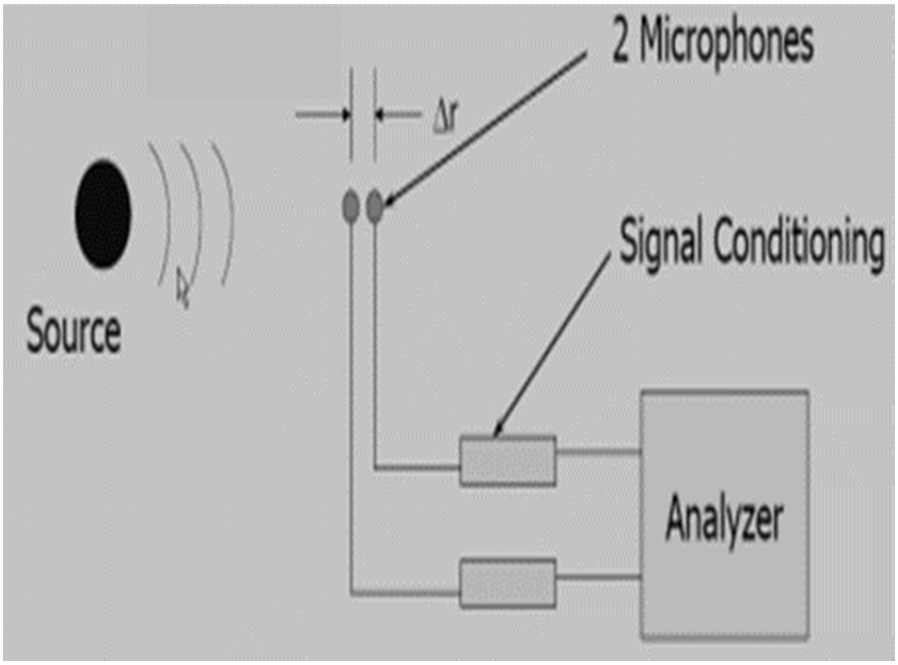

FIGURE 4.4: Schematics of OBSI Set-up (Analyzer and Computer in Vehicle)

Figure 4.4 shows the circuit from the analyzer to the microphones. The locations of the microphones correspond to the ends of the contact patch. The distance between microphones is also checked to ensure that leading edge and trailing edge effects are distinctively captured though they are ultimately averaged. The distance is also chosen to ensure that the likelihood of destructive interference was remote. The contact patch is characteristic of the SRTT and its inflation pressure.

After calibration, the next step was the operation of the sedan at an approach distance sufficient to acquire and maintain a cruising speed of 60 miles per hour through the test section to collect OBSI data for that section. Data was collected at a steady 60 mph speed in automatic 5-second sections (a distance of 440 ft.). Testing at 60 miles per hour was done for each run of each test. It was also possible to make continuous runs in contiguous test sections and crop the individual section data by identifying start (of section) and end

(of section) event markers. This method was much more efficient when care was taken to identify and match the cropped sections with test results.

A typical output from a test is shown in Table 4.1. With reference to Equation 3.4, the first column shows the sound intensity level (SIL) for each of the one-third octave frequencies from the leading edge microphone. The resulting OBSI for the leading edge is then calculated by application of Equation (3.4). Similar measurements and calculation for the trailing edge are shown in the third column of Table 4.1. A combined OBSI for the test is obtained by arithmetic average of the leading and trailing edge OBSI. The combined OBSI was later used in the analysis.

TABLE 4.1: Typical OBSI Output from One Run.

	SOUND INTENSITY (dBA)		
FREQUENCY (HZ)	**LEADING EDGE**	**TRAILING EDGE**	**AVERAGE**
400	86.2	85.7	86.0
500	86.8	88.6	87.8
630	90.5	89.7	90.1
800	95.1	93.5	94.4
1000	93.7	93.8	93.7
1250	93.8	94.9	94.4
1600	93.7	93.8	93.7
2000	92.8	92.5	92.7
2500	89.3	88.6	89.0
3150	83.4	83.5	83.4
4000	80.0	79.2	79.6
5000	76.6	75.6	76.1
A-WEIGHTED	103.0	102.8	102.9
OBSI			

4.3: OBSI DATA

Testing over the four-year period generated a very large database. The total data set included 582 individual OBSI measurements. Of these, however, only 433 were

associated with both a corresponding IRI and temperature value. This data set is used in refining the suggested OBSI model of Chapter 3. For the purposes of this presentation this data is arranged as follows. First, it is recognized that there are eight distinct surface finish configurations (see Table 4.2); the associated normalized geometric values (see Equations 3.18 a and b) for each of these finishes are listed in Table 4.2.

TABLE 4.2: Distinct Texture Configurations

TEXTURE TYPE	CONFIGURATION #	ASP (mm)	ASPGW (mm)	DIR	SP	MPD (mm)
Transverse Tine	1a	15	6	1	0	0.81
	1b	18	6	1	0	0.85
Traditional Grind	2	6	3	0	1	0.91
Innovative Grind	3	15	3	0	0	1.21
Ultimate Grind	3*	15	3	0	0	1.19
Exposed Aggregates	4	9	9	1	1	0.7
Broom/Turf Drag	5a	3	2	0	1	0.39
	5b	3	2	1	1	0.34

Then, for each of the surfaces the measured OBSI values against normalized temperature (Equation 3.19) and normalized IRI (Equation 3.20) are listed in Table 4.3. The actual IRI in this data ranged from 1.2 m/km to 4.09 m/km and covers the common range of pavement smoothness generally encountered in a large network. In addition, the testing temperature ranged from -8 ^{o}C (265 $^{\circ}$K to 37^{o}C (310 $^{\circ}$K). These measurements,

representing the most comprehensive set of tire noise measurements obtained to date, will be used in the next Chapter to identify the appropriate model form of Chapter 3.

The ranges (maximum-minimum) and mean values of the OBSI for each surface type were calculated and this data is summarized in table 4.3. Two observations are made on the data in Table 4.3. The analysis of this table leads to two observations:

1) The differences in the mean OBSI values of ~6 dBA might indicate the expected spread of noise levels associated with different surface texturing.

2) On the other hand, the range within each texture type, which takes values from 0 to ~7 dBA, indicates that the noise contributions from temperature, IRI, and measurement error are of the same order as those for surface texturing. That is surface texture variables may have as much influence on determining tire-pavement interaction noise (OBSI) as environmental conditions (temperature) and ride quality (IRI). This same conclusion can also be drawn by making a cumulative frequency plot for the texture types with sufficient data (Figure 4.5). If confirmed by the proposed model, this will open up a promising design option for developing quieter pavements.

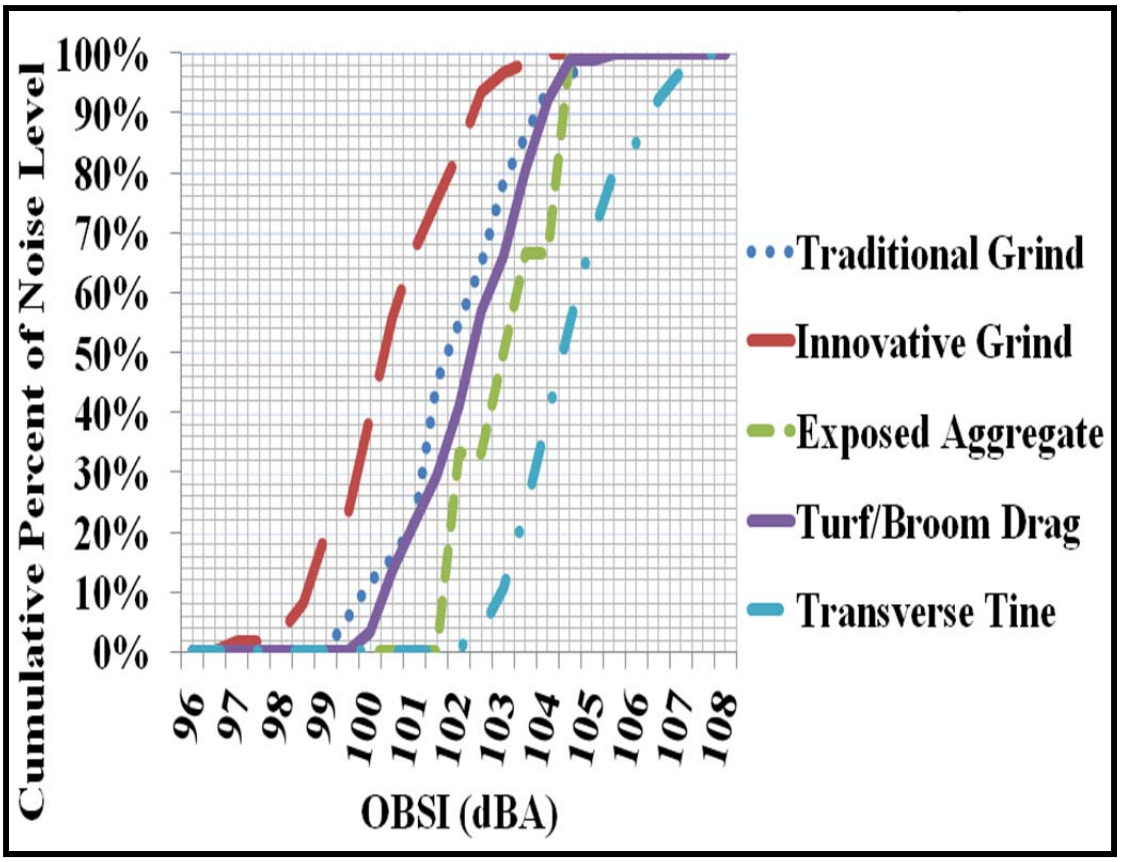

FIGURE 4.5: Cumulative Percentile OBSI Data Measured (Data Currently Includes IRI and Temp Effects)

TABLE 4.3: Descriptive Statistics of the 433 Sample Space OBSI Data

	Transverse Turf	Transverse Tine 1a	Transverse Tine 1b	Exposed Aggregate	Turf/Broom Drag	Traditional Grind	Innovative Grind	Innovative (Ultimate) Grind
Mean	105.39	104.47	103.17	103.02	102.25	101.87	100.46	98.33
Minimum	104.60	102.00	100.54	101.63	99.57	99.02	96.88	96.80
Maximum	106.94	107.40	104.60	104.46	105.27	104.66	103.62	98.90
Range	2.34	5.40	4.06	2.83	5.70	5.64	6.74	2.10
Count	4	160	32	6	88	84	61	4

TABLE 4.4a Temperature IRI and OBSI of Configuration 1a Transverse Tine

TEMP	IRI (m/km)	OBSI (dBA)
256.23	1.42	105.15
256.63	1.64	107.16
258.37	1.34	104.5
263.37	1.67	106.37
263.45	1.63	104.9
267.99	1.51	105.8
269.35	1.52	105.1
269.35	1.23	103.8
271.29	2.65	103.25
271.29	1.60	103.15
273.04	1.38	104.71
273.06	3.05	107.35
273.07	2.29	106.7
273.07	2.41	107.2
273.07	2.86	107.1
273.08	2.86	107.35
273.08	1.57	106.64
273.09	1.98	103.34
273.09	2.08	104.7
273.1	2.65	106.7
273.13	1.22	106.7
273.14	1.22	104.3
273.2	0.65	103.49
275.74	1.43	104.47
276.05	1.50	104.35
279.98	1.79	103.47
279.98	1.67	105.33
280.29	1.24	103.7
256.23	1.42	105.15
256.63	1.64	107.16
258.37	1.34	104.5

TABLE 4.4b: Temperature IRI and OBSI of Configuration 1b Transverse Tine

TEMP (T) (^{o}K)	IRI (m/km)	OBSI (dBA)
275.07	1.40	103.81
275.07	1.26	104.15
275.07	1.4	103.88
278.6	1.58	104.06
278.6	1.25	104.05
278.6	1.44	103.93
283.38	1.34	102.99
284.39	1.37	103.98
284.39	1.25	104.15
284.39	1.27	103.8
284.39	1.17	102.83
288.3	1.10	100.58
291.05	1.10	104.18
291.05	1.22	104.6
291.05	1.47	103.9
291.48	1.37	102.74
291.48	1.25	103.15
291.48	1.27	102.56
291.48	1.17	100.83
292.62	1.28	103.53
293.05	1.54	102.94
293.05	1.28	103.61
293.05	1.47	102.28
296.5	1.28	102.8
296.5	1.44	102.5
296.93	1.58	102.55
296.93	1.25	103.13
296.93	1.44	102.68
298.07	1.21	100.54
298.43	1.35	103.8
298.43	1.24	103.24
298.43	1.27	103.57

TABLE 4.4c: Temperature IRI and OBSI of Configuration 2 Conventional Grind

TEMP (^{o}K)	IRI (m/km)	OBSI (dBA)
256.23	1.10	101.30
256.63	1.10	101.65
256.63	1.18	102.56
258.37	1.34	104.50
258.37	1.74	102.50
258.9	1.72	101.93
263.37	1.04	101.55
263.37	1.10	102.17
263.45	1.07	101.00
267.44	0.69	101.32
267.44	1.68	102.88
267.99	1.37	102.20
268.27	0.75	101.18
269.35	1.52	105.10
271.09	0.83	100.73
271.09	0.64	100.55
271.09	1.04	102.98
275.74	1.06	99.80
275.74	1.11	101.05
276.05	0.71	99.88
276.05	1.32	101.50
278.17	0.64	99.75
278.36	0.77	99.48
278.36	1.24	101.12

TABLE 4.4d: Temperature IRI and OBSI of Configuration 3 Innovative Grind

Temp (^{o}K)	IRI (m/km)	OBSI (dBA)
275.43	1.21	101.20
277.30	1.33	99.97
277.87	1.84	100.24
278.60	1.13	100.10
278.60	1.13	100.08
282.67	1.10	100.50
284.39	1.17	101.97
284.39	1.17	102.03
286.50	1.21	101.31
286.50	1.21	100.89
287.03	1.47	100.82
287.63	1.38	101.13
288.30	1.10	100.70
288.30	1.10	100.40
290.95	0.87	100.00
291.05	1.33	100.89
291.05	1.33	99.93
291.48	1.17	99.77
291.48	1.17	100.07
295.94	1.08	99.87
296.20	1.82	99.50
296.20	1.82	99.70
296.28	1.02	98.90
296.93	1.13	99.50

TABLE 4.4e: Temperature IRI and OBSI of Configuration 3*: Ultimate Innovative Grind

TEMP (^{o}K)	IRI (m/km)	OBSI (dBA)
277.3	0.95	98.9
277.87	0.93	98.7
278.6	0.95	96.8

TABLE 4.4f: Temperature IRI and OBSI of Configuration 4: Exposed Aggregate

TEMP (^{o}K)	IRI (m/km)	OBSI (dBA)
290.95	1.431	103.00
290.95	1.780	103.00
298.55	1.289	101.62
298.75	1.667	101.58

TABLE 4.4g: Temperature IRI and OBSI of Configuration 5a. Longitudinal Drag

TEMP	IRI (m/km)	OBSI (dBA)
275.43	1.25	103.31
298.75	1.24	102.18
290.95	1.20	104.35
291.09	0.62	99.58
287.03	0.91	102.63
296.28	0.62	101.02
300.83	0.68	100.02
282.75	0.68	101.77
275.01	0.91	101.98
298.55	0.90	101.95
290.95	0.87	104.08
273.13	1.76	102.49
273.15	2.45	102.60
273.12	2.89	100.85
273.12	2.40	101.33
273.12	1.87	101.33
273.16	1.67	101.33
273.08	1.72	104.97
273.16	2.19	105.07
273.11	1.63	105.14
273.15	1.24	102.60
273.11	1.42	102.96
273.08	1.64	103.08
273.09	1.04	103.08

TABLE 4.3h: Temperature IRI and OBSI of Configuration 5b: Transverse Drag

TEMP (^{o}K)	IRI (m/km)	OBSI (dBA)
273.07	1.72	104.97
273.16	2.19	105.07
273.11	1.63	105.14
273.15	1.24	104.60

4.4: CHAPTER SUMMARY

The OBSI method of tire pavement noise measurement measures tire pavement noise at the noise source. It is thus preferred to other noise evaluation methods and used in this study.

Variation of OBSI of various configurations indicates that by changing a surface texture configuration acoustic properties may be altered also. This fact may be useful in design of quiet pavements. At the same time, variability in OBSI data within each texture type indicates that other variables extraneous to texture may also be significantly affecting OBSI. Temperature and IRI cannot therefore be ignored.

CHAPTER 5: FITTING THE MODEL

5.1 CHAPTER INTRODUCTION

The objective of this chapter is to find the best of the candidate models for tire pavement interaction noise from Chapter 3 and identify the "best fit" parameters using the field data of Chapter 4. Recall from chapter 3 that, in normalized form, the two candidate models to be fit are

$$\text{a) } \mathrm{OBSI} = \mathrm{A} + \mathrm{BT} + \mathrm{C\ IRI} + [(\mathrm{ASP})(\mathrm{D\ x\ DIR} + \mathrm{E})] + [(\mathrm{MPD})(\mathrm{F\ x\ DIR} + \mathrm{G})] + [(\mathrm{SP})(\mathrm{J\ x\ DIR} + \mathrm{K})] \quad (5.1)$$

Alternatively, using asperity groove width ASPGW* as defined in Chapter 3

$$\text{b) } \mathrm{OBSI} = \mathrm{A} + \mathrm{BT} + \mathrm{C\ IRI} + [(\mathrm{ASPGW}^{*})(\mathrm{D\ x\ DIR} + \mathrm{E})] + [(\mathrm{MPD})(\mathrm{F\ x\ DIR} + \mathrm{G})] + [(\mathrm{SP})(\mathrm{J\ x\ DIR} + \mathrm{K})] \quad (5.2)$$

Where for completeness it is noted that the variables that have been defined in Equations 5.1 and 5.2 with the asterisk now removed are:

ASP = normalized asperity grove width
MPD = normalized mean profile depth
SP = spikiness (a categorical variable 0 or 1)
DIR = direction (a categorical variable 0 or 1)
IRI = normalized International Roughness Index
T = normalized temperature

Fitting the model requires three tasks:

- The identification of significant variables,
- Elimination of insignificant variables and
- Determination of the "best" fit coefficients.

The method used to achieve this is a stepwise regression method [SRM] [5.1] that performs the 3 steps listed above. Provided below is an overview of the SRM including detail on how significant variables are selected and best fit values obtained.

5.2: OVERVIEW OF STEPWISE REGRESSION METHOD

The method used to fit the candidate models with the data is a stepwise regression method, which involves either of two strategies known as the additive strategy and the subtractive strategy. The subtractive stepwise regression analysis used in this work began with all the starting variables (Table 2.1) and observed the characteristics and goodness of the fit with the F- test [5.1]. Subsequent steps included various combinations of variables and a corresponding observation of their adjusted coefficient of determination. The adjusted coefficient of determination is an unbiased measure of goodness of fit and will increase only if a significant variable is added to the model. As this is not necessarily true for coefficient of determination, the (unadjusted) coefficient of determination is not deemed adequate for phenomenological models.

To facilitate the process of elimination of inadequate combinations of variables, the confidence level was set to 95% such that models with variables exhibiting p-values higher than 0.05 were summarily considered insignificant. P-value is a measure of how much evidence we have against the null hypothesis (H_o). The null hypothesis states that there is no relationship between a dependent variable and the independent variable or that the variable does not have any significant effect on the model. However, a failure to reject the null hypothesis is not the same as acceptance of the alternate hypothesis, H_a. The smaller the p-value, the more evidence we have against H_0 [5.1]. It is also a measure

of how likely we are to get a certain sample result or a result "more extreme," assuming H_0 is true.

5.3: RESULTS

Most research work using OBSI [1.7] have used 95% confidence level as a standard for significance. This level of significance corresponding to a confidence level of 95% does not allow a "Type I" error more than 5% occurrence. A "Type I" error occurs when one rejects the null hypothesis whereas it is true. Usually a one-tailed test of the hypothesis is used in association with a "Type I" error. Additionally, a key reference [5.4] recommends a significance of 0.05 when dealing with large data and stepwise regression.

The statistical package, Statistix 9.0 [5.2] facilitated the valuation of models based on combinations of variables. (ranging from single variables to all starting variables) to determine the significant variables and best fit model. Subsequently, Statistix 9.0 ran various combinations of the variables. By gradual elimination of insignificant variables based on the criteria outlined earlier, the process identified (at 95% confidence level), corresponding p-values of each variable and the corresponding mean sum of squared errors, the adjusted coefficient of determination of the model as well as model coefficients. The initial result was the model coefficients and goodness of fit values for all the initial variables (Table 5.1). That combination indicated (but not conclusively) which variables are significant variables. At that stage, the model coefficients were as expected, affected by the assignment of values to the insignificant variables, thus increasing the sum of squared residuals.

TABLE 5.1: Result of Initial Run of Model With all Identified Variables

MODEL WITH ASP		
Adjusted R^2		0.533
	Coefficients	P-value
Intercept	82.435	5.5E-110
T	19.236	1.1E-12
ASP	-0.003	0.009227
DIRASP	1.083	3.18E-40
MPD	-9.987	0.381992
DIR-MPD	0.173	0.63056
DIR-SP	0.542	0.301888
IRI	-0.494	0.03606
SP	-0.089	0.007

MODEL WITH ASPGW		
Adjusted R^2		0.227
	Coefficients	P-value
Intercept	84.258	3.63E-76
GDT	19.203	9.62E-08
ASPGW	0.003	0.008021
DIR-ASPGW	-0.199	0.431234
MPD	-14.024	0.12138
DIR-MPD	-0.118	0.88237
DIR-SP	0.896	0.266682
IRI	1.220	0.806
SP	0.285	0.048303

The resulting equation for the model after fitting the model form shown in Equation 5.1 was as follows:

$$\text{OBSI} = 99.023 + 20.164\left(\frac{293 - \text{T}}{\text{T}}\right) + \left[\left(\frac{\text{ASPT}}{\text{ASP}}\right)(1.513\ \text{DIR} + 0.098)\right] 5.849\left(\frac{\text{IRI}}{\text{IRIT}}\right) + 1.684\ \text{SP} \quad (5.3)$$

This is shown on the left side of Table 5.2 where all the p-values are less than 0.05

TABLE 5.2: Coefficients, P-Values and Adjusted R^2 of Final Model

Adjusted R^2		0.65
	Coefficient	P-value
Intercept	99.023	8.9E-142
T	20.164	4.06E-15
IRI	5.849	0.000226
DIR*ASP	1.513	1.1E-46
ASP	0.098	0.001162
SP	1.682	8.37E-13

Adjusted R^2		0.35
	Coefficients	P-value
Intercept	86.653	4.5E-42
T	15.689	3.06E-15
IRI	9.964	0.005
DIR*ASPGW	1.091	0.023
ASPGW	0.002	0.048
SP	5.043	0. 050

The alternative model using asperity groove width (Equation 5.2) when fitted turned out to be:

$$\mathrm{OBSI} = 86.653 + 15.689\left(\frac{293 - \mathrm{T}}{\mathrm{T}}\right) + \left[\left(\frac{\mathrm{ASPGWT}}{\mathrm{ASPGW}}\right)(1.091\ \mathrm{DIR})\right] + 9.964\left(\frac{\mathrm{IRI}}{\mathrm{IRIT}}\right) + 5.043\ \mathrm{SP} \quad (5.4)$$

This is shown on the right hand side of Table 5.2. The ASPGW-DIR variable appears to be significant but all others exhibited a p-value higher than 0.05.

Plotting the predicted versus measured OBSI using ASP [Equation 5.1], lines at 1.5 dBA offset were drawn parallel to the model line. These lines enclosed more than 90 percent of the data points. P-values were all <<0.05 in each of the five significant variables. Each set of surface data types were evidently not skewed across the model line in. In particular, each of the configuration types were equally scattered above and below the model line. This indicated that component texture types are in consonance with the proposed model and that the model is not unduly confounded by any of the texture types (Figure 5.1). The insignificant variables were MPD, DIR, MPD and DIRSP. Their p-values were each greater than 0.05. (See Tables 5.1 and 5.2).

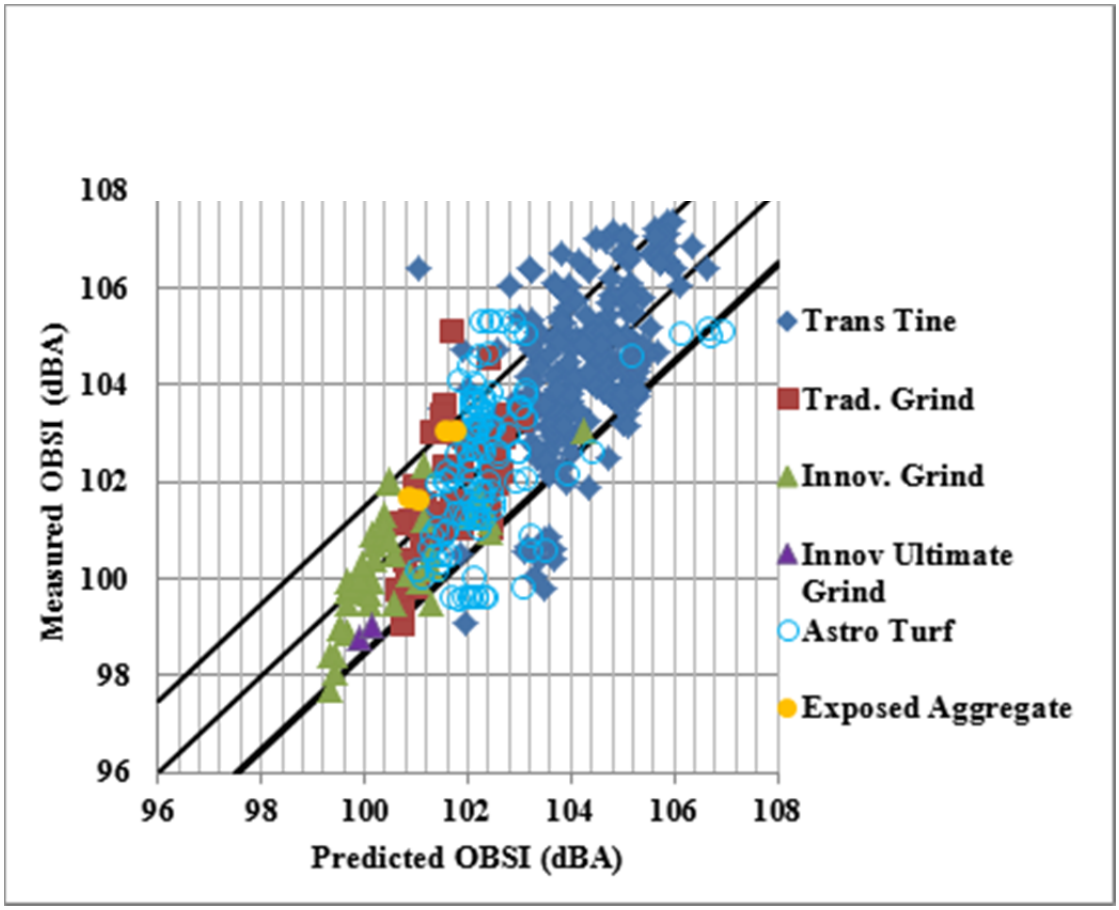

FIGURE 5.1: Fitted Model (1.5 dB Offset Enclosed 92% of the data)

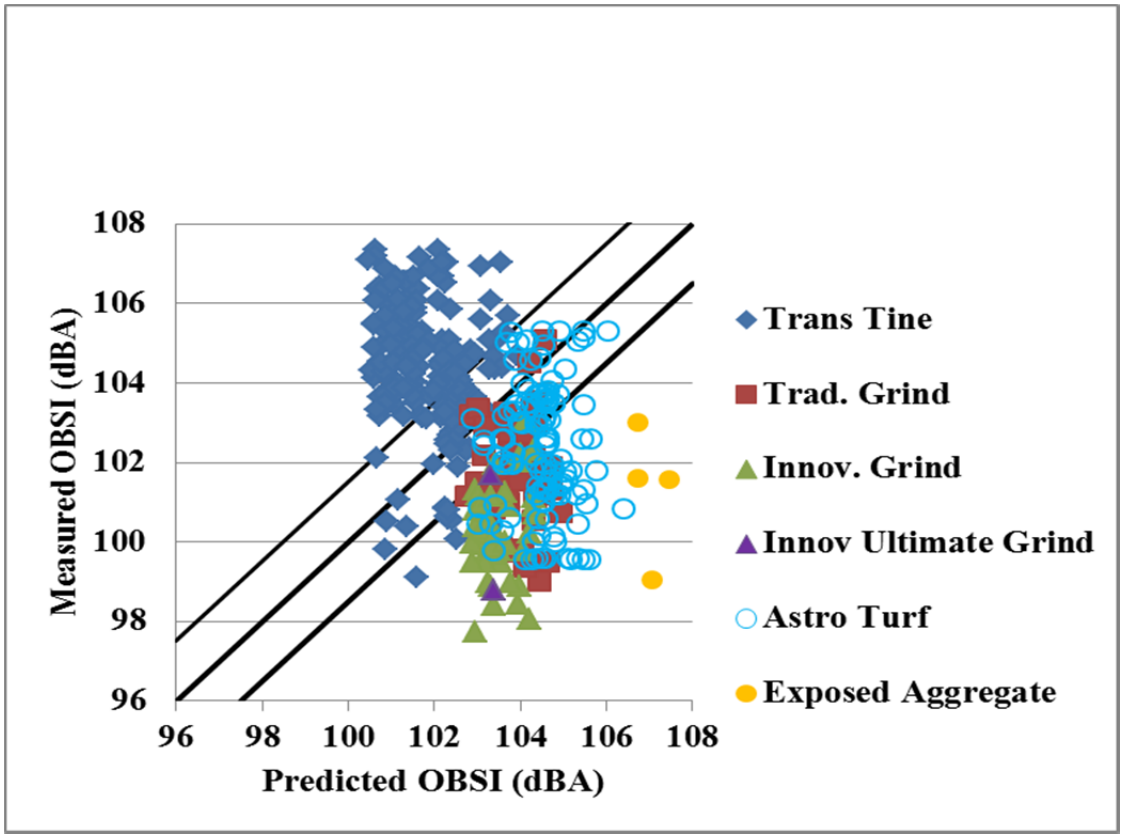

FIGURE 5.2: Model Obtained by Using Asperity Groove width in Lieu of Asperity Interval

The alternative equivalent using the ASPGW instead of ASP (Equation 5.2) had a higher mean sum of square errors (Table 5.2). The same variables were significant in each model but there was a significant attenuation (coefficient ≈ 0) of ASPGW. Moreover, P-values for ASPGW and SP are only slightly less than 0.05 though the mathematical value of the SP coefficient became unusually high. Although the variables were significant ($P<<0.05$), the alternative model retained only 25% of the data within the 1.5 dBA band of the model line.

Therefore, the alternative model based on the ASPGW does not appear to be nearly as reliable as the model Equation 5.1 that is based on ASP. The model also predicts that larger groove width results in higher noise levels and that transverse tine is quieter than

the diamond grinding configuration and exposed aggregate is noisiest, without temperature and IRI normalization (Figure 5.2).

Consequently, the use of ASP (Equation 5.1) shows that was therefore a much better fit than Equation 5.2 that used ASPGW. Figure 5.1 suggests that the process successfully identified the leading variables in determining OBSI. The model identified asperity interval, mean profile depth (MPD) (ASTM E- 2157) and other composite variables (DIRSP and DIR MPD) as being of little or no significance. When any combination of these variables are added to the proposed OBSI model (Equation 5.1) in the stepwise regression, their associated p-values fell in the range $p > 0.1300$ indicating that they exhibited little or no-significance in modeling the OBSI. Those variables were thus considered insignificant by the chosen model based on the confidence level.

Finally the chosen model after many steps was:

$$\mathrm{OBSI} = 99.023 + 20.164\left(\frac{293 - \mathrm{T}}{\mathrm{T}}\right) + \left[\left(\frac{\mathrm{ASPT}}{\mathrm{ASP}}\right)(1.513\ \mathrm{DIR} + 0.098)\right] + 5.849\left(\frac{\mathrm{IRI}}{\mathrm{IRIT}}\right) + 1.684\ \mathrm{SP} \quad (5.3)$$

5.4: COMPARISON OF PREDICTED OBSI RANGE OF MODEL COMPONENTS

Generally, the model (Equation 5.1) predicted OBSI from 98.5 dBA to 106.5 dBA, which is similar to the range of data measured (98 to 107 dBA). However, it is expedient to accentuate the contribution of the components of the model (significant variables) to the overall OBSI by examining their contributed data range and corresponding range of OBSI in the model. This is shown in Table 5.3.

TABLE 5.3 Effect of Component Variable on the Model

OBSI CONTRIBUTION				
COMPONENT	**MIN (dBA)**	**MAX (dBA)**	**RANGE (dBA)**	**SOURCE VARIABLE**
$\mathbf{5.849}\left(\frac{\mathbf{IRI}}{\mathbf{IRIT}}\right)$	0.25	1.87	1.62	Min and Max IRI are 0.65 and 4.8 m/km respectively
$\mathbf{20.164}\left(\frac{\mathbf{293-T}}{\mathbf{T}}\right)$	-0.78	2.11	2.89	Min and Max Temp are 265 K and 305 K
1.68 SP	0	1.68	1.68	Min and Max SP are 0 and 1 respectively
$\left[\left(\frac{\mathbf{ASPT}}{\mathbf{ASP}}\right)(\mathbf{1.513\ DIR\ +0.098})\right]$	0.15	5.1	4.96	Max and Min DIR are 0 and 1 respectively

Table 5.3 shows the range of contribution of each variable to the prediction model based on its sub –model-form. The largest range is exhibited by texture direction and asperity interval compound variable (4.96 dBA). This is followed by temperature (2.89 dBA), then by spikiness (1.68 dBA), and then by IRI (1.62 dBA). This table will be found useful in investment planning towards quiet pavements. For example if it is only a change in direction that will be achieved through the texturing, the acoustic benefits can be predicted in comparison to a change in SP or ASP or both, using this table.

5.5: VALIDATION OF NORMALITY & HOMOSCEDASTICITY

A tenable model development process also requires re-examination the model a-posteriori for homoscedasticity and normality of the residuals. One of many ways of testing normality is to perform the normality plot (FIGURE 5.3). This follows the process of Shapiro-Wilk [5.2], [5.3]. It plots a statistic of ordered values versus "RANKIT". RANKITS are the expected values of the ordered statistics of a sample from the standard normal distribution the same size as the data. The coefficient of determination of the distribution plotted against the corresponding normal distribution was 0.98. This shows that the distribution can be approximated to a normal distribution. Figure 5.4 presents a tenable validation of homoscedasticity of residuals.

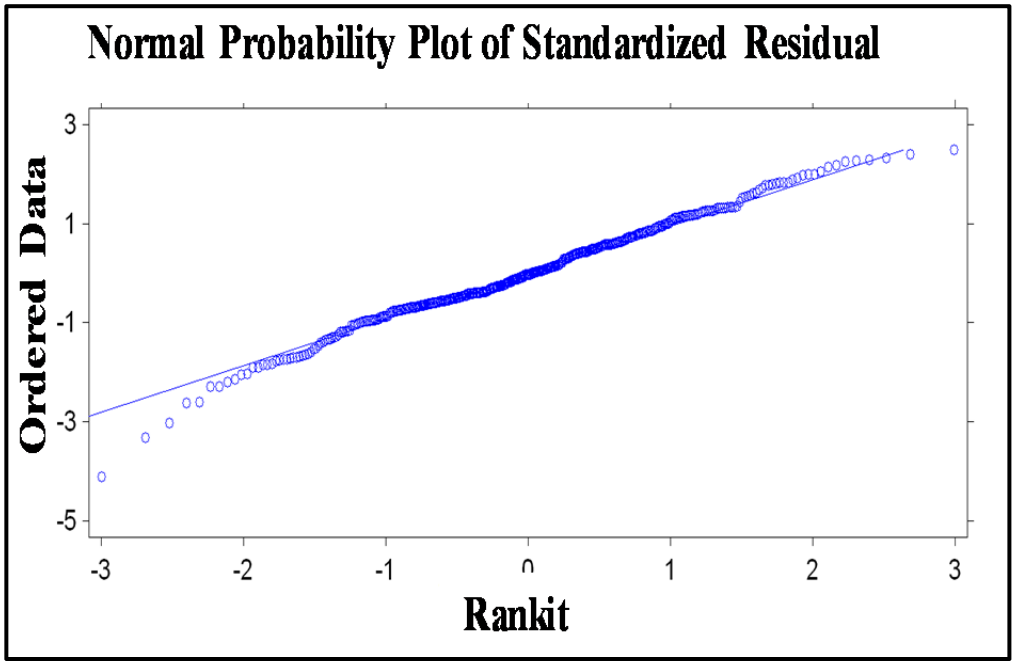

FIGURE 5.3: Normality of the Residuals by Plot of Ordered Data vs. Rankits

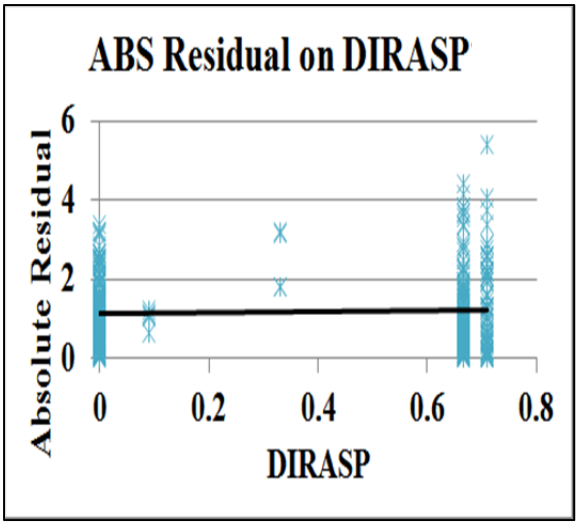

Homoscedasticity of DIRASP Residuals

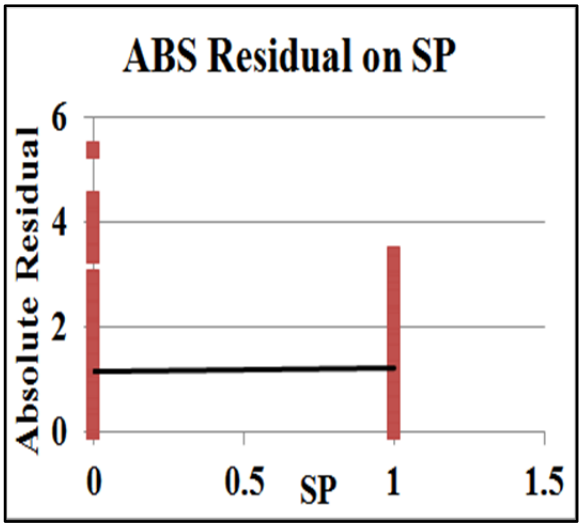

Homoscedasticity of SP Residuals

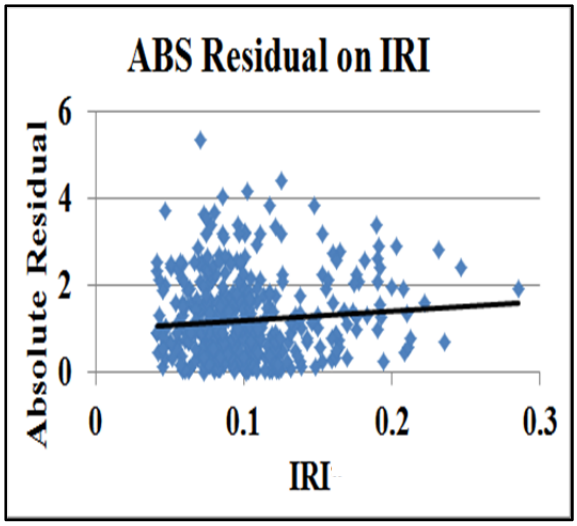

Homoscedasticity of IRI Residuals

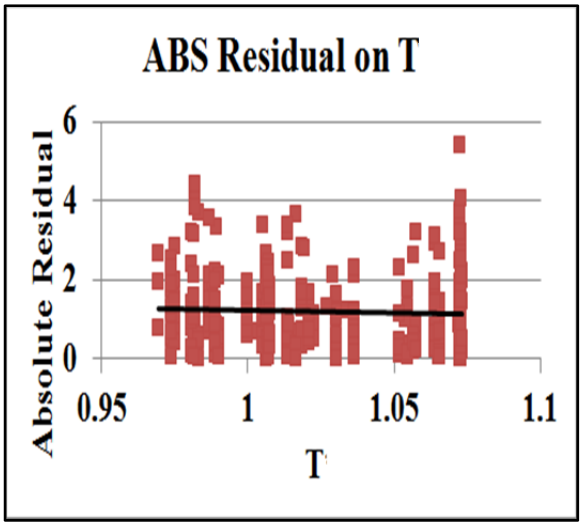

Homoscedasticity T Residuals

FIGURE 5.4: Homoscedasticity Validation in the Model

5.6: POWER OF MODEL

Statistical significance α and the statistical power (1- β) are associated with a function, f (α , β) [5.3] where β is the probability of obtaining a "Type II" error in a model. These parameters can be combined with standard deviation (σ) of the population and the

number needed to detect a change, (δ), to produce the required sample size. The required sample size for a given set of α , β, σ and δ was determined as follows:

$$S = 2\frac{\left(Z_{\propto} + Z_{1-\beta}\right)^2 \sigma^2}{\delta^2} \tag{5.5}$$

Where

S is the required sample size

$Z_{\propto}$ is the Z statistic for the significance

$Z_{1-\beta}$ is the Z statistic for the model power

σ is standard deviation of OBSI data

δ is the number needed to detect a change in OBSI (1dBA)

According to AASHTO TP 76-09, it is customary to expect that 1 dBA is sizeable enough to detect a change in noise level. The standard deviation from the data is computed to be 3.169. $\left(Z_{\propto} + Z_{1-\beta}\right)$ values were obtained from statistical tables. Consequently, at a 95% confidence limit and to be 80% certain of the correlation (α = 0.05, β= 0.2, f (α , β) = 2.8) requires 150 data points. Thus a data set larger than 150 will be necessary for an adequate sample space. For a 95% certainty, S= 249.

It is therefore evident that, for the dataset with 433 combinations of OBSI versus IRI, ASP, SP, TEMP, and DIR, the power of the regression is > 95%. This is tenable for research level and project level predictions in similarly controlled environments. It will also provide tenable predictions in large networks of pavement infrastructure where data is collected in an environment not necessarily as controlled as the research facility where this study was conducted.

5.6: CHAPTER SUMMARY

A phenomenological model based on the identified variables appears to predict OBSI considering that 90% of the data is enclosed within a 1.5 dBA offset. For convenience the model is shown here:

$$\mathrm{OBSI} = 99.023 + 20.164\left(\frac{293 - \mathrm{T}}{\mathrm{T}}\right) + \left[\left(\frac{\mathrm{ASPT}}{\mathrm{ASP}}\right)(1.513\ \mathrm{DIR}\ + 0.098)\right]$$
$$5.849\left(\frac{\mathrm{IRI}}{\mathrm{IRIT}}\right) + 1.684\ \mathrm{SP}$$

It can be seen that the model validates the hypothesis that the prediction model should contain small scale texture variables as well as large scale texture variables (IRI) and an environmental variable: temperature. In selecting the variables, the difference between using ASP and ASPGW shows that the variables in the model cannot easily be replaced by other geometric variables without the consequence of upsetting the model.

The model variables are ranked based on the practicable range of their component in the model from the most influential to the least influential accordingly:

1) Asperity interval and direction compound model variable
2) Temperature
3) IRI and Spikiness.

The model does not violate the requirement for homoscedasticity, normality of residuals and linearity. The power of the model was examined and found to be >90 % based on the data size. Statistical methods used in this research have been discussed and the main criteria for significance, P-value for individual variable and adjusted coefficient of

determination for the model, have been elucidated. The next chapter discusses an important implication of the model.

CHAPTER 6: IMPACT OF SURFACE TEXTURE ON NOISE

6.1: STRATEGY

Many practitioners want to know which pavement surfaces irrespective of non-texture variables are quieter for the same non-texture-related conditions. The pavement noise model described in Chapter 5 (Equation 5.1) can be readily used to answer this question by simply assuming a constant temperature (T) and a constant ride quality (IRI). This way, the influences of variables extraneous to the texturing are removed from the prediction model. For such an analysis, the IRI of 1 m/km was chosen, as that will be encountered in a new pavement surface without faulting and serious built in warp and curl. A temperature of 293 $^{\circ}$ K was chosen in consonance with the European Union Commission [6.1] pivot for their stepped temperature correction algorithm.

For convenience typical parameters for various textures are shown in Table 6.1. A plethora of model predictions is obtained by entering these dimensions into the model (Equation 5.3) with IRI set to 1 and temperature set to 293 $^{\circ}$ K. Figure 6.1 shows comparison of the predicted OBSI vs. measured OBSI based on this strategy. Figure 6.1 shows a model OBSI of 100.3 dBA at the lowest noise level (left hand side of the plot) for the innovative grind textures. At the upper end of the range side of the plot, this model shows that an OBSI of 105.3 dBA is typical for transverse drag texturing. These results clearly show that the spread in intrinsic pavement noise is ~ 5 dBA (well within human detection).

Figure 6.1 can now be examined and discussed. The group furthest to the left in Figure 6.1 is entirely made up of the innovative grind texturing. In this category, all textures have a negative spikiness and a longitudinal direction: a situation that removes the 5th term and a significant part of the 4th term of Equation 5.1. The size of the 4th term is

lowered further by the fact that this texturing has a constant and high asperity interval (ASP= 15 mm).

TABLE 6.1: The Dominant Configuration Dimensions in the Model

VARIABLE		Ultimate Innovative Grind	Innovative Grind	Conventional Grind	Longitudinal Drag	Transverse Tine	Transverse Tine	Exposed Aggregate	Transverse Drag
ASP INTERVAL (mm)		16	15	6	4	15	18	8	3
DIR Longitudinal =0 Transverse =1		0	0	0	0	1	1	1	1
SPIKINESS Non-Spiky=0 Spiky =1		0	0	0	1	0	0	1	1
Noisy Features	ASP→0	-	-	x	x	-	-	x	x
	Transverse	-	-	-	-	x	x	x	x
	Spiky	-	-	x	x	-	-	x	x

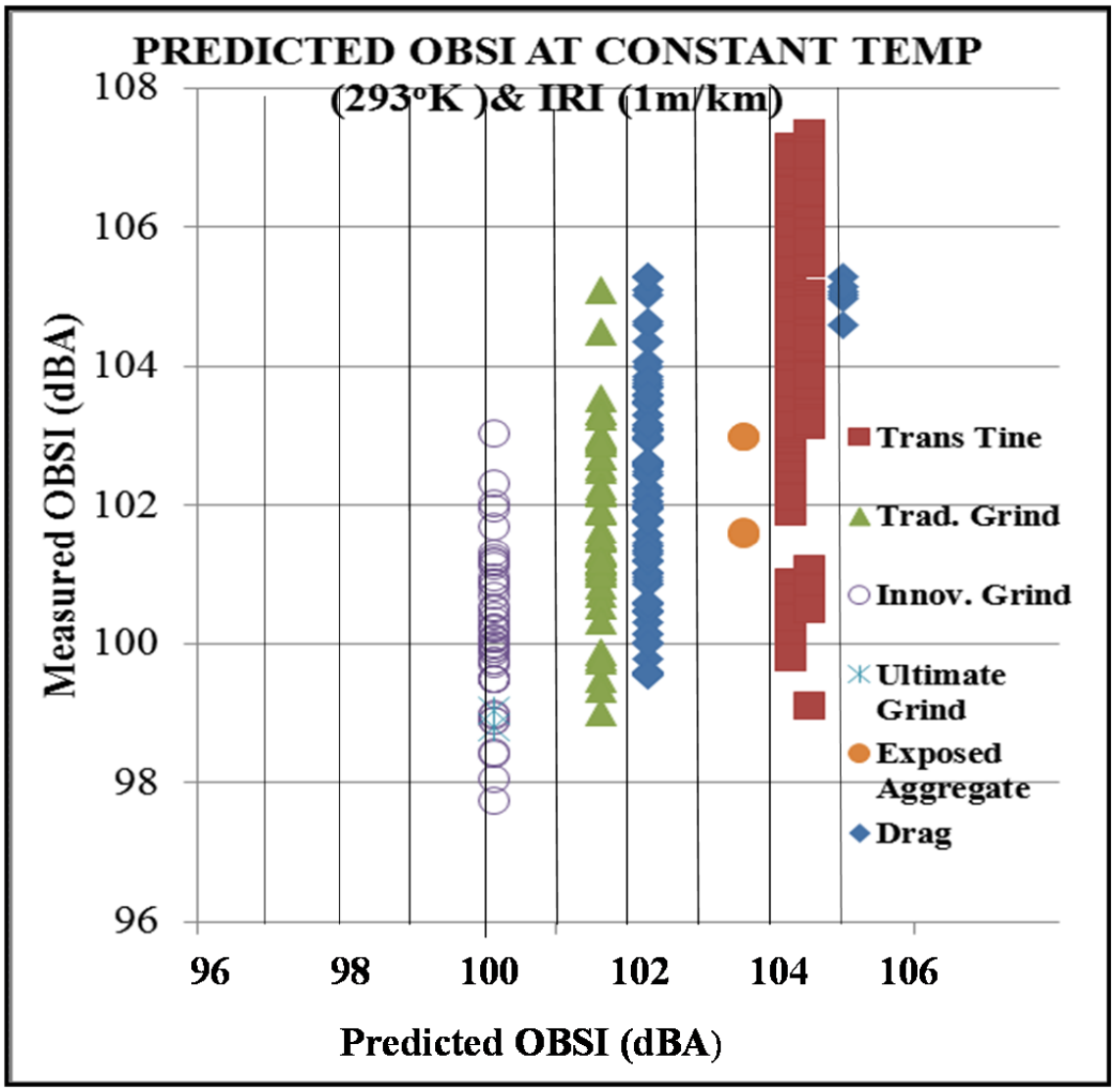

FIGURE 6.1: Predicted Vs. Measured OBSI at IRI of 1 m/km and Temperature of 293 °K

The next group to the right is made up of the traditional grind and drag textures. This shift is provided by the reduced asperity interval (6 mm for conventional diamond grind) as well as the positive spikiness. The slight difference in the results of the 2nd group is due to a different asperity interval (ASP of drag texture = 3 mm versus ASP of conventional grind texture = 6 mm). The second subgroup of drag textures (transverse

drag) is separated from the first group of drag textures (longitudinal drag) by effect of direction clearly to form another group.

The third group is made up of transverse tine and exposed aggregate textures. The jump in noise here is due to texture direction. In this group also is the noisiest sub-group which appears to be the transverse drag in which spikiness and small asperity interval combine to predict a very noisy pavement. It appears that investing in direction alone may be more beneficial than investing in a combination of spikiness and asperity interval. That can be the plausible reason why transverse tine with only one noisy attribute remains one of the noisiest textures.

6.2: CHAPTER SUMMARY

This exercise showed that for the same environmental condition, the surface textures can be ranked from quietest group to noisiest group in the following order: innovative grind in the first group, longitudinal turf drag and traditional grind in second group and exposed aggregate, transverse tine and transverse drag in the third group.

CHAPTER 7: APPLICATION OF THE MODEL IN REHABILITATING A SURFACE TO REDUCE NOISE

7.1: BRIEF BACKGROUND

A phenomenological model for OBSI prediction was developed in Chapter 5. Chapter 6 discussed how texture types based on the model would affect on-board sound intensity noise. This Chapter describes how the prediction model was applied towards achieving quiet pavement in two rehabilitation projects in Minnesota.

Projects included Interstate 94, a 1000-ft stretch at approximately at mile post 190 near Monticello Minnesota and approximately the last10 miles of Interstate 35 in Duluth, Minnesota. Interstate 94 originally had a turf drag texture, while the Duluth Interstate 35 project originally had the transverse tine texture. Both were rehabilitated by diamond grinding because reduction of tire-pavement noise was one of the objectives of the rehabilitation. This project provided an opportunity to validate the model described in Chapter 5.

7.2: VALIDATION PROCESS

The following activities were conducted.

1) Texture configurations, IRI, and OBSI prior to rehabilitation were measured for each of the projects.
2) The OBSI was predicted for each section and compared with measured OBSI.
3) Texture design for quiet pavement was performed and specification for IRI.
4) Texture configurations were developed.
5) After diamond grinding was performed, IRI and OBSI were measured. The predicted and measured OBSI were compared.

Step 1: Pre-grind measurements: Texture, IRI, and OBSI were measured prior to the rehabilitation. The results of these measurements are shown in Table 7.1. Table 7.1 shows that the pre-grind textures were noisy and were thus candidate for quiet pavement projects.

TABLE 7.1: Pre-Grind Measurements.

	I-35		I-94	
Pre-Grind Measurements	**Northbound**	**Southbound**	**Northbound**	**Southbound**
ASP (mm)	13	13	3	3
DIR	1	1	0	0
SP	1	1	1	1
IRI (m/km)	2.5	2.5	2.5	2.5
Temp($^{\circ}$K)	288	288	295	295
Measured OBSI (dBA)	106.1	105.2	103.2	103.2

Step 2: Evaluation of OBSI model for the prior-to-rehabilitation section: Data in Table 7.1 were used to predict pre-grind OBSI using Equation 5.1. Table 7.2 shows a comparison of the predicted and measured OBSI for each pavement section. It can be observed that for each case the pre-grind predicted OBSI are within 1 dBA of the measured OBSI.

Table 7.2: Model Prediction versus Measured OBSI Pre-Grind

Model Component to Measured Pre-Grind	Northbound Pre Grind (Duluth)	Southbound Pre Grind (Duluth)	Northbound Pre Grind (St. Cloud)	Southbound Pre Grind (St. Cloud)
Measured OBSI (dBA)	106.1	105.2	103.2	103.2
Predicted Pre-Grind OBSI	105.1	105.1	102.4	102.3
Measured – Predicted OBSI (dBA)	0.95	0.05	0.85	0.85

Step 3: Design or rehabilitation of surfaces: Based on Equation 5.1, a quiet pavement strategy includes ensuring that DIR=0 and SP=0 and large asperity intervals (ASP). Based on these guiding principles, the following surface configuration specification (was developed:

- Longitudinal direction (DIR=0)
- Negative surface texture (no spikiness) (SP=0)
- Asperity interval, ASP, = 16 mm
- Post-rehabilitation roughness IRI = 1 m/km

Using Equation 5.1, for the ambient temperature of 293 ºK, the target OBSI for the post rehabilitation surfaces was 99.89 dBA which is significantly lower than the measured pre-rehabilitation OBSIs.

To achieve this configuration, the surface was ground in 2 stages, first a flush grind to reduce bumps and reduce IRI to prescribed values. It was followed by the grinding to the

configurations specified. The process of diamond grinding was described in Chapter 2.

Step 4: Post – rehabilitation evaluation: After the rehabilitation was performed, IRI and OBSI were measured for each test section. Table 7.3 presents the results of the measurements along with the Equation 5.1 OBSI for the ambient temperatures at the time of IBSI measurements. One can observe that the predicted post grind and measured post-grind OBSI were within 1 dBA,

TABLE 7.3: Texture Design For Grinding

	DULUTH (I-35)		**ST. CLOUD (I-94)**	
	Northbound	**Southbound**	**Northbound**	**Southbound**
ASP (mm)	16	16	16	16
DIR	0	0	0	0
SP	0	0	0	0
IRI (m/km)	0.75*	0.75	1.2**	1.05
Temp (°K)	290	290	298	298
Predicted Post Grind OBSI (dBA)	99.7	99.7	99.3	99.3
Measured Post Grind OBSI (dBA)	99.7	99.3	98.7	98.2

*Target OBSI was 0.8m /km. **Target OBSI was 1 m/km.

Final Quiet Grind Configuration 3

Original Transverse Tine (Configuration 1a)

FIGURE 7.1: The Quiet 2010 Ultimate Grind and the Pre-Grind Transverse Tine

7.3 CHAPTER SUMMARY

Application of the phenomenological model resulted in noise reduction in two projects in Minnesota. In each project the predicted OBSI for the pavement surface before and after rehabilitation were in each case within 1 dBA of the predicted OBSI. The two rehabilitation project thus provided validation of the model. An elaborate analysis of

acoustic performance of certain concrete surface configurations was discussed and provided by Izevbekhai and Khazanovich [7.2].

CHAPTER 8: CONCLUSION & RECOMMENDATIONS

8.1 SUMMARY OF RESEARCH EFFORTS

This research investigated tire pavement interaction noise to determine the associated significant parameters and created a phenomenological model predicting tire pavement noise from these variables.

- By identification of possible contributors to tire-pavement noise towards proposing a model form for prediction it characterized pavement surfaces variables from small scale features related to texture and the larger scale features related to ride quality.
- It developed and utilized a protocol for collecting tire-pavement noise and texture related as well as IRI data from various test sections.
- This research used the proposed model form, data collected and rigorous statistical techniques to develop a model for predicting tire-pavement interaction noise from surface texture, ride quality and environmental (air temperature) inputs.
- It validated this model in two rehabilitation projects by successfully predicting OBSI to within 1 dBA of the measured value.

8.2: SPECIFIC CONTRIBUTIONS OF THIS RESEARCH

This study conceptualized and investigated the variables that may be correlated to on board sound intensity, derived the model forms, validated the model with data and applied the model for a quiet texture design. Other specific contributions include the following:

Successful development of model-forms by first successfully identifying significant variables: The hypothesis of total OBSI being made up of components of small scale texture, large scale texture and temperature implications led to successful identification of the relevant variables within these groups.

A tenable method for quantifying spikiness (SP): In developing the phenomenological model some miscellaneous contributions included determination of a tenable method for quantifying spikiness for use in noise prediction. This method based on amplitude distribution function was an improvement over traditional methods of determining negative and positive textures.

A phenomenological tire pavement noise prediction model: A phenomenological model predicting OBSI from identified texture variables, IRI and temperature was produced by fitting the curves using the large data set of measured values, and derived model-form.

Relative importance of model components: Based on range of configurations and dimensions examined, the relative contribution of each variable components and range in the OBSI prediction model has been demonstrated. This can guide an agency on how to direct their investments towards quiet pavements.

8.3: CONCLUSIONS

Prior to this research, mean texture depth (and by implication, mean profile depth) was thought to be an important variable for the prediction of OBSI TPIN (Tire Pavement Interaction Noise). This research has shown that MPD may not have significant correlation to OBSI in the data examined.

Prior to this research work, there was little or no recognition of the importance of asperity interval or an understanding of its importance in tire pavement interaction noise. Texture

asperity interval was found to be influential to OBSI showing a decrease in OBSI with increasing asperity interval.

Prior to this research, there was no OBSI predictive model that included IRI, although there was conventional wisdom among practitioners that the roughness effects cannot be ignored. This research work provided for the first time an OBSI predictive model that included International Roughness Index (IRI), confirming that increased IRI resulted in increased OBSI. Sensitivity of IRI to seasonal variations may be inconsequential in ride quality measurements but the influence on OBSI is significant.

Prior to this research work, there was no omnibus sound intensity surface characteristic model composed of explanatory variables that belong to three main categories: the pavement surface parameters, pavement ride comfort, and climatic factors. This research provides that robust model.

Asperity-interval and temperature were found to be negatively correlated to OBSI, while IRI, texture-spikiness and texture direction were positively correlated to OBSI. Consequently, the model validates the hypothesis that transverse textures, positive texture-spikiness and pavement roughness increase tire pavement noise while larger asperities and higher temperature decrease OBSI.

The study successfully applied the quiet pavement model to design the texture for two rehabilitation project in Minnesota. Predicted and measured OBSI were significantly similar. The model is not only mathematically tenable but physically verifiable.

By examination of noise generation mechanisms and analysis of a point source element subjected to a pulsating noise source, it was shown that sound intensity depends on components of the source (amplitude and angular speed), as well as on environmental variables (density and speed of sound) pertaining to the medium. OBSI was shown to be

correlated to a reciprocal of temperature. Relative humidity and atmospheric pressure were observed to be not significantly correlated to OBSI and were not therefore analyzed further.

8.4: RECOMMENDATIONS

As a subject for future research, a detailed study of the variability of OBSI data is paramount. Going forward, further studies should include a time series analysis when the newer sections would have had many cycles of testing sufficient for an autoregressive modeling with de-trending.

This research identified tread block impact and air compression relief as leading noise generation mechanisms but did not distinctly quantify the noise levels for each. It is recommended that in further research the OBSI is fragmented into low and high frequency components and redesigned to produce outputs accordingly. The low frequency impacts of the tread block and the higher frequency impacts of the air pumping relief may then be safely identified and evaluated.

To improve the model, it may be necessary to investigate discrete or continuous alternatives to the categorical variables of texture direction and spikiness.

8.5: LIMITATIONS OF THE STUDY

All the observation and conclusions drawn from this experiment were based on measurements conducted and data obtained from the MnROAD test sections. This experiment is limited by constraints in typical values for the variables measured and analyzed. OBSI typically ranges from 95 to 112 dBA and the predictive models may not apply to values outside of this range irrespective of the mathematical feasibility of such

projections. Similarly, MPD analyzed in this experiment are within typical ranges of 0 to 2.5 mm. Since rumble strips are much deeper (9 mm - 25 mm) than typical textures, extrapolating results from this model to rumble strips may not be tenable.

Results from this research may not be applicable to flexible pavements as the viscoelastic variable will probably be introduced and analyzed in that case, or to pervious concrete where acoustic impedance may be of consequence. The model may require more variables to evaluate pervious pavements and flexible pavements.

The novelty of the OBSI method as well as the new sections and absence of winter season testing data (limited by equipment guidelines) currently inhibits time series analysis of OBSI.

REFERENCES

1.1 Ulf Sandberg Tire/road noise –Myths and realities Plenary paper published in the Proceedings of The 2001 International Congress and Exhibition on Noise Control Engineering The Hague, The Netherlands, 2001 August 27–30

1.2 Ulf Sandberg U I-INCE Working Party on Noise Emissions of Road Vehicles (WP–NERV) Convener of the I-INCE Working Party on Noise Emissions of Road Vehicles. Swedish National Road and Transport Research Institute SE-581 95 Linköping, Sweden. (Final report produced with the assistance of Working Party members International Institute of Noise Control Engineering 2001)

1.3 Sorensen M, Hvidberg M, Andersen ZJ, Nordsborg RB, Lillelund KG, Jakobsen J., Tønneland, A., Overvad, K., Raaschou-Nielsen O Road traffic noise and stroke: a prospective cohort study. Eur Heart J. 2011 Mar; 32(6):737-44. pub 2011 Jan 25

1.4 United States Department of Transportation. Federal Highway Administration Safe, Accountable, Flexible, Efficient Transportation Equity Act: A Legacy for Users (SAFETEA-LU). Office of Legislation and Intergovernmental Affairs Program Analysis Team. http://www.fhwa.dot.gov/safetea-u/summary.htm. Accessed 9/19/09.

1.5 United States Department of Transportation FHWA Highway Traffic Noise CEQ. 40 CFR Section 1508.12: Terminology: Federal agency. Code of Federal Regulations. 6/17/10.

1.6 United States Department of Transportation FHWA. “Noise Barriers.” Highway Traffic Noise. http://www.fhwa.dot.gov/environment/noise/noise_barriers. Accessed 10/5/10.

1.7 Rasmussen, R., Bernhard, R.J., Sandberg, U., Mun, E.P., The Little Book of Noise. U.S. Department of Transportation Federal Highway Administration. FHWA-IF-08-004. July 2007. Shrouds James M. U.S. Department of Transportation Memorandum.

1.8 Bernhard, R.J., McDaniel, R. Noise Generation for Pavement Engineers. Transportation Research Record: Journal of the Transportation Research Board of the National Academies. ISSN 0361-1981 Issue Volume 1941 / 2005.

1.9 Rochat J.L Highway traffic measurements on acoustically Hard Ground compared to the Predictions from the Traffic Noise Model Portland, Maine U.S. Department of Transportation, Volpe Center Acoustics Facility 55 Broadway, DTS-34, Cambridge, MA 02142, USA NOISE-CON 2001 2001 October 29-31

2.1 Izevbekhai, B.I. Akkari A. Performance of Exposed Aggregate Surface under High Volume Traffic. Paper submitted to Journal and presented at ASTM International E-17 Symposium. Dec 2011. Publication in Progress

2.2 Wu C, Nagi, M.A. (1995) "Optimizing Surface Texture of Concrete Pavement" Portland Cement Association Research and Development Bulletin RD111T 1995.

2.3 Snyder, M.B., "Pavement Surface Characteristics: A Synthesis and Guide. ACPA Publication EB235P. American Concrete Paving Association. 2007

2.4 ASTM E 2157 -02. Standard method for determining Mean Profile Depth using the Circular Track Meter. URL www.astm.org . Assessed 5/30/2009

2.5 ASTM F 2493-08 (2008). Standard Specification for P225/60R16 97S Radial Standard Reference Test Tire. www.astm.org . Assessed 5/30/2009

2.6 Hamet, J.F, Klein, P. Road Texture and Tire Noise. INRETS, 25 av. F. Mitterrand F69675, Bron, France. http://www.inrets.fr/ur/lte/publications/publications pdf/web -hamet/in00_674.pdf. Accessed 4/20/2010.

2.7 Whitehouse D.J. A Handbook of Surface Nanometry Second Edition Taylor and Francis US 2009

2.8 ISO 4287:1997 Geometrical Product Specifications (GPS) -- Surface texture: Profile method -- Terms, definitions and surface texture parameters. International Standards Organization.

2.9 Izevbekhai, B.I., Khazanovich , L., & Voller, V. Development and Validation of a Phenomenological Model for Tire-Pavement Interaction noise. Transportation Research Board CD ROM. January 2012.

2.10 Sayers, M.W., Gillespie, T. D., and Paterson, W.D. Guidelines for the Conduct and Calibration of Road Roughness Measurements, World Bank Technical Paper No. 46, The World Bank, Washington DC, 1986.

2.11 Byrum, C. R. (2001). A High Speed Profiler Based Slab Curvature Index for

Jointed Concrete Pavement Curling and Warping Analysis, Doctoral Dissertation, University of Michigan.

2.12 Karamihas, S.M., T.D. Gillespie, R.W. Perera, and S.D. Kohn. 2001. Diurnal changes in profile of eleven jointed PCC pavement. Proceedings of 7th International Conference on Concrete Pavements, Orlando, FL.

2.13 Khazanovich, L., M.I. Darter, R. Bartlett, and T. McPeak. 1998. Common Characteristic of Good and Poorly Performing PCC pavements. Technical Report FHWA- RD- 97-131, McLean, VA: Federal Highway Administration, Turner-Fairbanks Highway Research Center.

3.1 Rasmussen, R.O., Bernhard, R.J., Sandberg, U., Mun, E.P. (2007) The Little Book of Quiet Pavements. U.S. Department of transportation FHWA-IF-08-004. July 2007.3.2

3.2 AASHTO TP 76-11. (2011) Standard Method of Test for Measurement of Tire/Pavement Noise Using the On-Board Sound Intensity (OBSI) Method.

Sound Intensity URL http://physicsx.pr.erau.edu/Courses/CoursesS2010. Accessed 5/12/2010.

3.3 Sengpiel E. Form Zur Mikrofonaufnahmetechnik und Tonstudiotechnik URL:http://www.sengpielaudio.com Assessed 5/20/10 Wiley Interscience, 1992.

3.4 The Engineering Toolbox Resources, Tools and Basic Information for Engineering and Design of Technical Applications URL http://www.engineeringtoolbox.com Assessed 12/1/2009

3.5 Directive 2002/49/EC of the European Parliament and the Council of 25 June 2002 Relating to Assessment and Management of Environmental Noise. Official Journal of the European Communities 18.7.23002. URL http://eur-lex.europa.eu/LexUriServ/LexUriServ.do?uri=OJ:L:2002:189:0012:0025:EN:PDF

3.6 Klein P, Hamet. J.F. An envelopment Procedure for Tire Road Contact. Technical Report SILVIA_INRETS-009-WP2 INRETS

3.7 Wu C, Nagi, M.A. “Optimizing Surface Texture of Concrete Pavement” Portland Cement Association Research and Development Bulletin RD111T 1995.

3.8 Izevbekhai, B.I. & Vaughan V.R. Development and validation of a tenable process

for quantifying texture spikiness for pavement noise prediction. International Journal of Pavement Engineering Taylor and Francis DOI:10.1080/10298436.2012.698013, June 2012

4.1 Hanson D. I., Waller B Evaluation of Noise Charactreristics of Minnesota Pavements National Center for Asphalt Technology (NCAT) Auburn University Auburn Alabama 2005.

4.2 AASHTO TP 76-09. American Association of State Highway Transportation Officials AASHTO Interim Guidelines for the Measurement of On Board Sound Intensity (OBSI) of Pavements

4.3 AASHTO TP 76-11. American Association of State Highway Transportation Officials AASHTO Interim Guidelines for the Measurement of On Board Sound Intensity (OBSI) of Pavements:

4.4 Pierce, A.D. "Causality and mathematical models in vibration and acoustics, a realistic perspective," Proceedings of Meetings on Acoustics, Vol. 5, Issue 1, 2008.

4.5 Pierce A. D. Acoustics: An Introduction to its Physical Principles and Applications (American Institute of Physics, New York, 1989).

4.6 Rasmussen, R.O., et al. "Identifying Quieter Concrete Pavements using On-board Sound Intensity." Transportation Research Board Annual Meeting, Washington, Bruel & Kjaer Sound Intensity Primer. (1990) Bruel & Kjaer DK-2850. Denmark.

4.7 Newland D.E Random Vibration, Handbook of Noise and Vibration Control, Ch. 13, 205- 211, Wiley, New York 2007.

5.1 Chatterjee, A. (2006) FHWA. National Highway Institute Scientific Methods of Research. FHWA - NHI-03-127 Course #123002.

5.2 Statistix 9.(2006) User Manual and Analytical Software. P.O Box 12185, Tallahassee, FL 32317-2185.

5.3 Devore, J.L. Probability and statistics for Engineering and the Sciences Fourth Edition 1995 Wadsworth Publishers Belmont CA 94002 ISBN 0-534-24264-2

5.4 Ji, Zhen; Shi, D., Li, Q and Wu, Q.H. Noise Reduction and Confidence Level Analysis in MMG-based Transient Fault Location. International Institute for Electrical Engineers Conference & Exhibition: Asia and Pacific Dalian, China 2005

5.5 Probability concepts in engineering Planning and Design Hua-Sing A. A & Tang, W.H - Wiley (2007) -

6.1 EU (2000) Opinion of the Commission Pursuant to Article 251 (2) Third paragraph Point(c) relating to motor vehicles amending Directive 92/23/EC. Document 500P0744. EU commission EUR-Lex) Brussels.

7.1 Izevbekhai, B.I. Wilde W.J. Innovative Diamond Grinding on MnROAD Sections 7, 8, 9, and 37 http://www.lrrb.org/pdf/201105.pdf Assessed 11/31/2009

7.2 Izevbekhai, B.I. & Khazanovich, L. Acoustic Enhancement of Concrete pavement Surface through Diamond. International.Journal of Pavement Engineering Taylor and Francis. DOI:10.1080/10298436.2012.690517 May 2012

A1.1 EU 2001/43/EC Directive 2001/43/EC of the European Parliament and the Council of 27 June 2001 on the Tires for Motor Vehicles and their Trailers and to their Fitting. The Official Journal August 4 2001.

A1.2 Konishi, S., Fujino, T., Tomita, S., Ozaki, T. Temperature dependency of Pass-by Noise. SAE Paper 971991, Society of Automotive Engineers Warrendale PA USA.

A1.3 AASHTO TP 76-08. American Association of State Highway Transportation Officials AASHTO Interim Guidelines for the Measurement of On Board Sound Intensity (OBSI) of Pavements

A1.4 Fahy F.J. Sound Intensity Second Edition 1995. Taylor & Francis ISBN-10: 0419198105.

A1.5 Kinsler L. E., Austin Frey, Alan B. Coppens James V. Sanders. Fundamentals of Acoustics. Third Edition 1980. John Wiley & Sons New York.

A1.6 Smith , D. Sound Intensity URLhttp://physicsx.pr.erau.edu/Courses/CoursesS2010 . Accessed 5/12/2010.

A1.7 Gade S. Technical Review 3-1982 Sound intensity Theory. Bruel & Kjaer DK-2850 Denmark

A1.8 Bruel & Kjaer Sound Intensity Primer. Bruel & Kjaer DK-2850 Denmark

APPENDIX: SOUND SOURCE AND ACOUSTIC MEDIA

APPENDIX 1A
ENVIRONMENTAL EFFECTS ON ON-BOARD-SOUND-INTENSITY LEVELS DERIVED FROM THE RESPONSE OF AN ACOUSTIC MEDIUM TO A PULSATING SOURCE IN CONTACT

Tire-pavement interaction noise is a combination of longitudinal waves with various frequencies. The noise is affected by many factors such as pavement surface characteristics, pavement conditions, tire characteristics, and vehicle speed. Empirical observations led to the conclusion that ambient conditions affect noise as well. Several researchers have proposed to correct pavement noise measurement results for the ambient air temperature [A1.1], [A1.2], but no theoretical justification of this correction has been found in the literature nor interim standards [A1.3]. This limitation is addressed in this appendix by obtaining an analytical relationship between the gas media properties and theoretical sound intensity by considering a one-dimensional illustrative example.

Consider the particular problem of one dimensional sound wave propagation through a gas cylinder. One end of the cylinder is subjected to displacement, Y_0, in the longitudinal direction with an amplitude A and circular frequency ω. The medium is assumed to be infinite, [A1.4] homogeneous and isotropic, where the density of the medium is denoted as ρ and speed of sound as c. For adiabatic conditions, the motion of a pulsating air mass resulting from the reciprocating motion of a source in contact under free field propagation is expressed as follows [A1.4]:

For a periodic wave the wave function is

$$Y(x,t) = \forall sin\left[\frac{2\pi}{\lambda}(x - vt)\right] \quad \text{(A1.1)}$$

where

$\frac{2\pi}{\lambda}$scales the wave to the natural period of the wave function. It is defined as k which is also called the wave number;

$\frac{2\pi v}{\lambda}$ is the angular frequency.

$\forall$ is the amplitude of the wave which is the maximum displacement of the wave.

Thus

$$y(x, t) = \forall \cos(kx - \omega t) \quad \text{(A1.2)}$$

where

y(x, t) is the displacement of the air particle located at a distance x from the source

ω is angular frequency

The wave number k can be defined as:

$$k=\omega/c \quad \text{(A1.3)}$$

From equation A1.4, the particle velocity, U which is not the speed of sound, can be written as

$$U(x, t) = \frac{dy(x,t)}{dt} = -\forall w\, sin(kx - \omega t) \quad \text{(A1.4)}$$

The pressure in the cylinder has the following form [A1. 6]:

$$P(x, t) = -\beta\frac{\partial y(x,t)}{\partial x} = \beta K \forall sin(kx - \omega t) \quad \text{(A1.5)}$$

where

β is bulk modulus. For gases the bulk modulus is related to the density and the speed of sound as follows:

$$\beta = \rho c^2 \quad \text{(A1.6)}$$

Sound Intensity is defined as follows [A1.3] [A1.7]

$$SI(x) = \frac{1}{\mathcal{T}}\int_0^{\mathcal{T}} PU dt \quad \text{(A1.7)}$$

Where

$\mathcal{T}$ is one period

Substitution of equations 4 and 5 gives based on [A1.5] and [A1.6]

$$SI(x) = 0.5\beta KA\ \frac{1}{\mathcal{T}}\int_0^{\mathcal{T}} (1 - cos2(kx - \omega t)\, dt = 0.5\ \beta k A^2\ \omega \quad \text{(A1.8)}$$

Substituting k=ω/c from equation A1.3 and $\beta = \rho c^2$ [A1.7] and [A1.8] from equation A 1.6,

$$\beta k = \rho\ c\ \omega \quad \text{(A1.9)}$$

Thus

$$SI = 0.5\ (\rho c)\omega^{\,2} A^2 \quad \text{(A1.10)}$$

Amplitude ∀ and angular frequency ω, are characteristics of the source, and thus do not depend on the acoustic medium.

From equation A1.8 the intrinsic tire noise can be expressed as

$$ITN \sim (\rho c)\omega^{2}\forall^{2} \qquad \text{(A1.11)}$$

Figure A 1.1 shows the variation of atmospheric pressure in the facility in which the test was conducted. It corroborates the fact that in the absence of drastic altitude changes associated with a noise data set, atmospheric pressure may not be a significant sound intensity variable. Similarly, the plot in Figure A1.2 indicates that the effect of relative humidity is insignificant in comparison to atmospheric pressure.

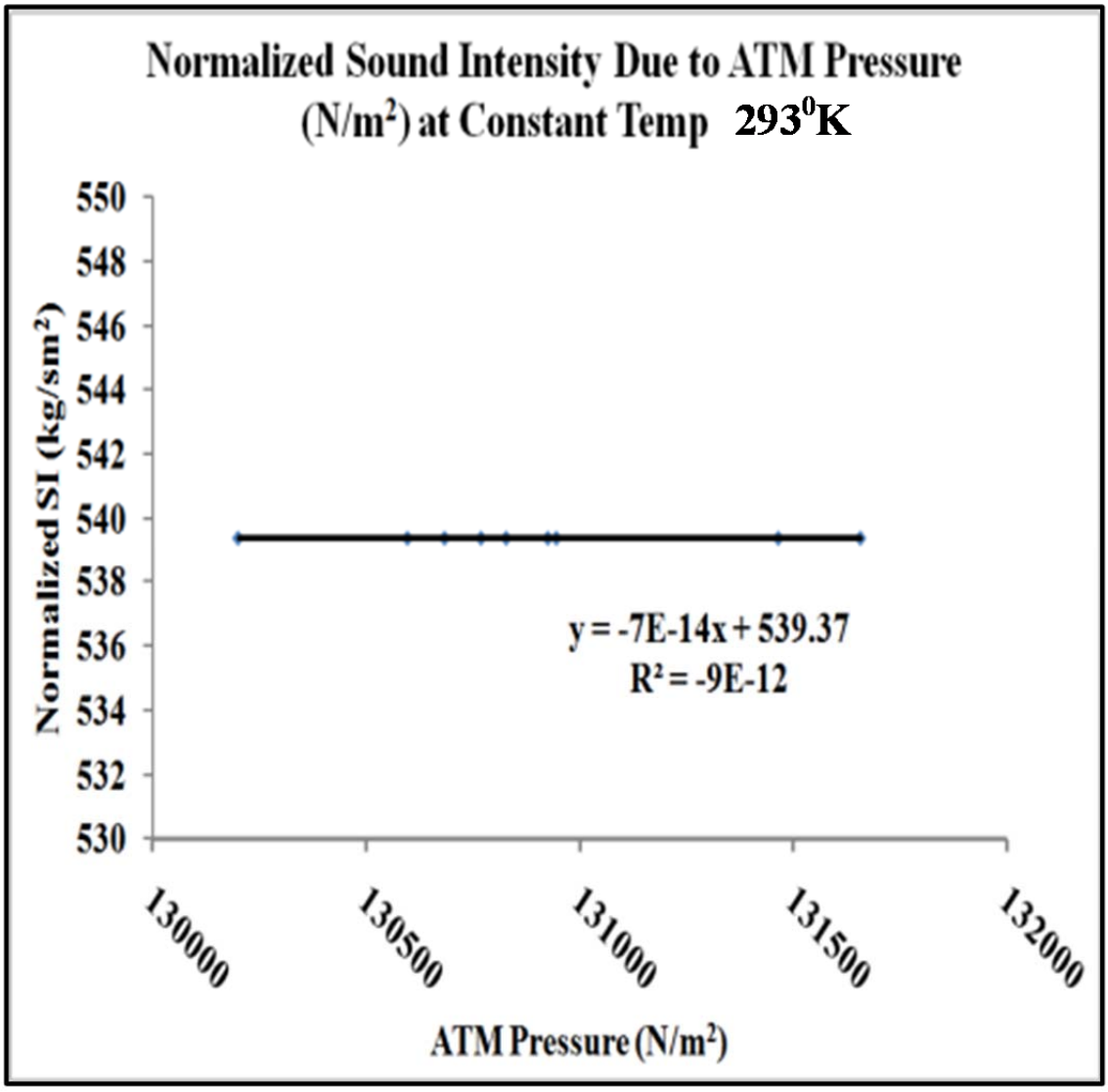

FIGURE A1. 1: Normalized Sound Intensity Due to Atmospheric pressure at MnROAD for Temperature of 293°K.

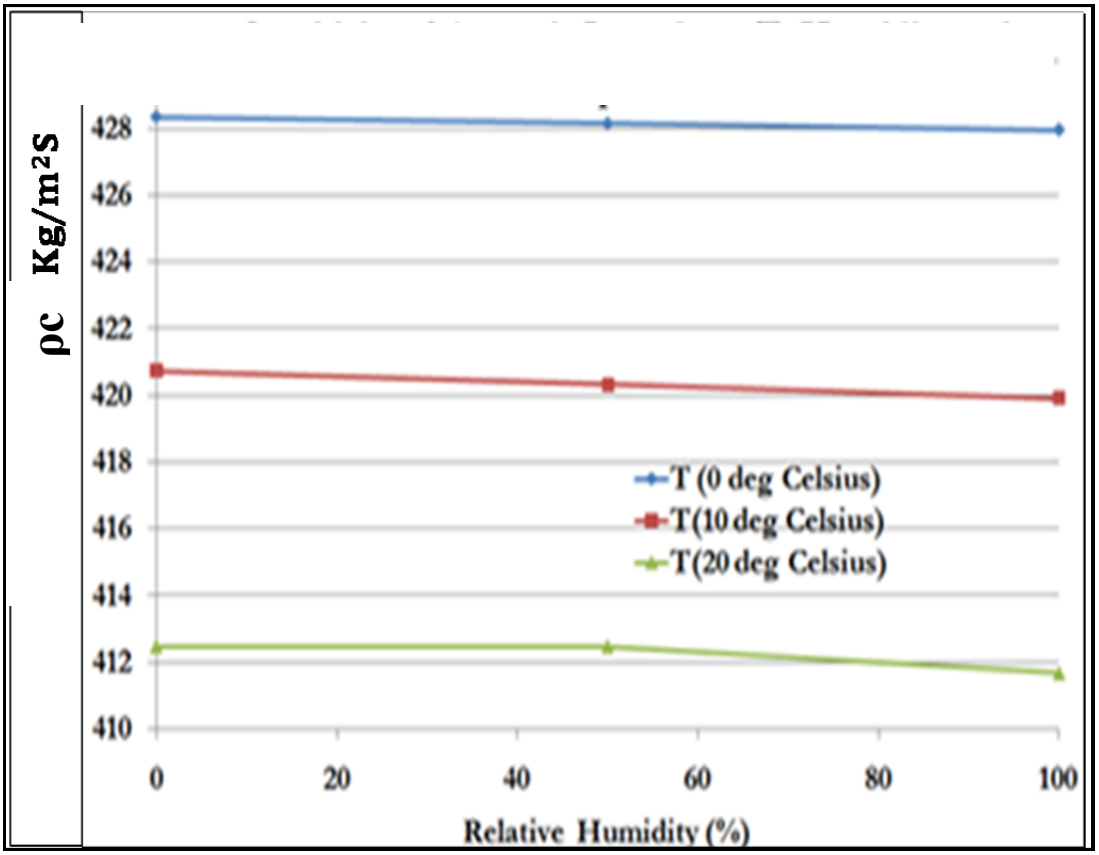

FIGURE A1. 2: Relative Humidity Effects on Normalized SI

It is evident from figures A1.1 and A 1.4 that temperature affects sound intensity. Pressure and humidity have very insignificant effect on sound intensity.

APPENDIX 1B: PRINCIPLES OF NEAR FIELD MICROPHONES (ACTIVE VS REACTIVE NOISE)

Sound pressure is defined as the fluctuation of the atmospheric pressure on account of sound energy emission and transmission. This disturbance commonly follows a rarefaction and compression pattern. Ordinarily, sound pressure is measured in Pascal or in N/m^2 [A1.7]. However sounds pressure level is defined as

$$SPL = 20 \log 10 \frac{P_1}{P_0} \quad \text{(A1.12)}$$

where P_1 is actual pressure in N/m^2 and P_0 is the pressure at threshold of human hearing. Sound pressure level is thus measured on the decibel scale as already described.

Sound energy is transmitted in an acoustic field or medium. Consequently, **sound intensity** is the more practicable description of the effect of a source on a medium. Sound Intensity is the rate of sound power dissipated or transmitted per unit area of the medium. Thus sound intensity will rapidly decline away from the source if the field is radially increasing in proportion to the inverse of the square of distance from the source. This results in what is known as the inverse square law of sound intensity.

$$SI_1/SI_2 = (d_2/d_1)^2 \quad \text{(A1.13)}$$

Since $$SI_{(i)} = \frac{\mathbf{P}}{\boldsymbol{\pi d_{(i)}^2}} (w/m^2) \quad \text{(A1.13B)}$$

It can be deduced that sound intensity follows the inverse square law.

However the sound intensity level is defined as

$$SI = 10 \log \left(\frac{SI_1}{SI_0}\right) \quad \text{(A1.14)}$$

where

SI_0 is the threshold sound intensity of 10E-12 Watts/m^2.

Sound source addition is a necessary process in acoustics. It provides a basis for logarithmic summation of sound intensity at various frequencies [A 1.4] and a basis to understand sound sources from dipoles and quadrupoles. However for the purpose of this research, the complexity of a moving source on a relatively uniform texture is idealized as a continuum of monopoles with summation of numerous leading, coincident and trailing effects. These are explained shortly. Similarly, for a simple monopole [A1.2] the sound pressure at a distance r is,

$$P(r,t) = i\rho_0 c \left(\frac{Qk}{4\pi r}\right)^2 \quad \text{(A1.14)}$$

where

$P(r, t)$ = pressure at a distance r and at time t [Pa]

ρ_0 = density of air [kgm^{-3}]

c = speed of sound in air [ms^{-1}]

ω = frequency [$rads^{-1}$]

t = time [s]

k = wave number [m^{-1}]

r = distance from center of source [m]

Q = source strength [m^3s^{-1}]

Q is also defined as:

$$Q = V(r)\, A(r) \text{ and } A = \pi d^2. \quad \text{(A1.15)}$$

where

A = Area of sphere

The average sound intensity at a radial distance r from a source is given by

$$SI(r) = \frac{1}{8}\pi \rho_0 c \left(\frac{Q}{\lambda r}\right)^2. \quad \text{(A1.16)}$$

where

λ= wavelength of sound.

Substituting for V and r,

$$SI(r) = 2\pi \rho_0 c(\omega r)^2 \text{ (watts/m}^2\text{)} \quad \text{(A1.17)}$$

This indicates that SI is a function of some atmospheric and pavement configuration variables. A similar derivation was made in the proceeding APPENDIX 1A. Sources add according to distance and intensity. Due to the waveform (Equation A1.18) constructive and destructive interference may occur on a micro scale when sound sources influence each other.

$$P(r, t) = \frac{\forall}{r} \exp i(\omega t - kr) \text{ and } U(r, t) = \frac{\forall}{w\varphi r}\left(k - \frac{i}{r}\right) \exp i(\omega t - kr) \quad (1.18)$$

where

φ= phase angle (rad).

There is a reactive and an active component of a generated sound field that influence how sources may interact. The difference between the active and reactive sound fields lies in the energy conservation process. The active field is a sound transmission field but the reactive field is the energy conversion field indicative of energy conversion into other forms. Fahy [A1.4] explained reactive field as the component of the solution to the general wave equation that mathematically represents the wave form that appears to be travelling into a source. The active components of the product of U and P (SI (r, t)) are expressed as:

$$\text{SI active (r, t)} = \frac{\forall^2}{\rho_o c w 2 r^2} \left(k - \frac{i}{r}\right) [1 + (\cos 2\ (\omega t - kr)] \quad \text{(A1.19)}$$

$$\text{SI reactive (r, t)} = \frac{\forall^2}{\rho_o w 2 r^3} \left(k - \frac{i}{r}\right) [\sin 2\ (\omega t - kr)] \quad \text{(A1.20)}$$

where

k is a wave number,

ω is angular speed, r is radial distance from source and t is time;

∀ is a complex amplitude parameter.

Tire pavement interaction noise is a near field measurement while statistical pass-by is a far field measurement. In a far field r is much greater than λ while the converse is true in a near field. It is evident that in near field, radiation is purely radial but the reactive component is quite influential since:

$$\frac{|SI_a|}{|SI_r|} = Kr \quad \text{(A1.19)}$$

where

SI_a is the active component of sound intensity and

SI_r is the reactive component of sound intensity.

The influence of the reactive field in near-field measurements affects the repeatability of tests. However the far field tests are fraught with errors that are accentuated with distance from the source. These include the different rates at which higher and lower frequency sources are diminished over distance. That being a more serious source of error renders the near field measurements more reliable. Moreover, while little or nothing can be done to influence other sources of noise apart from convoluted and labyrinthine legislative processes, the pavement texture variables can be controlled in design and construction especially as the definition of OBSI includes the frequency over which noise is

logarithmically summed. The on board sound intensity method based on American Association of State Highway and Transportation Officials (AASHTO) TP 76-09 performs this summation of sound intensity level over 12 one-third octave frequencies.